



# ESCUELA TÉCNICA SUPERIOR DE INGENIERÍA Y SISTEMAS DE TELECOMUNICACIÓN

## PROYECTO FIN DE GRADO

**TÍTULO:** HIGH-FIDELITY PIEZOELECTRIC LOUDSPEAKER

**AUTOR:** JAVIER FERNÁNDEZ MARTÍNEZ

**ESPECIALIDAD:** SONIDO E IMAGEN

**TUTOR:** DR. KEITH R. HOLLAND

**UNIVERSIDAD:** UNIVERSITY OF SOUTHAMPTON

**CENTRO:** INSTITUTE OF SOUND AND VIBRATION  
RESEARCH (ISVR)

**PAÍS:** REINO UNIDO

**Fecha de lectura:** 16 de Junio de 2014

**Calificación:**

**El Coordinador de Movilidad,**



Faculty of Engineering and the Environment  
Institute of Sound and Vibration Research

# High-fidelity piezoelectric loudspeaker

Javier Fernández Martínez

Supervised by Dr. Keith R. Holland

May 2014

This report is submitted in partial fulfilment of the requirements of the Degree of Acoustical Engineering, Faculty of Engineering and the Environment, University of Southampton.

---



## **Abstract**

This project reports on a literature review about piezoelectric loudspeakers and on an experimental research about how to improve some features of a particular horned piezoelectric tweeter.

The work involves an investigation of the performance and principle of operation of piezoelectric loudspeakers to understand how the sound is generated and what its main parameters are. Also, previous research papers about how to improve this type of speakers are reported.

The knowledge gained was used to reconsider and re-purpose a particular piezoelectric transducer. After characterising the original state of the device with acoustical and electroacoustical measurements, some improvements were implemented. Moreover, interesting conclusions were reached based on the results of the tests that were carried out. A structural study with a scanning laser was then completed. These sections demonstrated the need for providing the speaker with a rear suspension that guides the vibration of the membrane.

Finally, an inverse filter was designed in order to get a flat output response. After simulating the results with Matlab, validating experiments were run in the anechoic chamber with great success.



## Resumen

Este proyecto consta de un estudio detallado sobre piezoelectricidad y altavoces piezoeléctricos, así como de una parte experimental consistente en mejorar algunas características de un altavoz piezoeléctrico particular: un tweeter de bocina.

El estudio profundiza en cuáles son los principios de funcionamiento y los principales parámetros de este tipo de altavoces. Con el conocimiento adquirido a partir de trabajos de previos sobre el tema e investigación bibliográfica se ha llevado a cabo la parte experimental.

Esta parte ha requerido de una serie de medidas acústicas y electroacústicas para, primero, caracterizar el altavoz en su estado original y para posteriormente buscar y validar posibles mejoras, principalmente en la respuesta en frecuencia. Además, se ha realizado un estudio estructural del diafragma a partir de medidas tomadas con un vibrómetro laser Doppler. De estos tres procesos se concluyó que el altavoz bajo estudio tiene un problema en el soporte del cristal piezoeléctrico y se demostró la necesidad de equipar el dispositivo de una suspensión trasera que controle el movimiento del diafragma.

Finalmente, se ha diseñado e implementado en Matlab un filtro inverso, con el objetivo de conseguir una respuesta plana a la salida del altavoz. Su funcionamiento fue validado en la cámara anecoica satisfactoriamente.



## Acknowledgements

I would like to be grateful to everyone involved in making this project possible.

First of all, the biggest “thank you” is for my parents and my sister Laura. You can’t imagine how grateful I am for your support provided all through my degree, both in Spain and in the UK. This would have never come true without you. I am very happy to have you beside me in any decision that I made. You are a great pillar in my life.

I would also like to thank my supervisor Dr. Keith Holland, who gave me the opportunity to develop this project and always kept his door open to my enquiries.

A special gratitude to Jana for making easier the adaptation to Southampton and to Marcos for being always disposed to help me with the project. Also to my Erasmus friends and housemates; you have been of great help and encouragement throughout this year; I really appreciate having met you and became such good friends.

Thank you, to the rest of my friends and flatmates in León, Madrid and England. You know who you are; there is no need to name anyone.

*I wish I could transfer you  
all the energy used in doing this project, aunt.*

Javi.





# Contents

1. Introduction.....	13
2. Piezoelectric loudspeaker.....	14
2.1. Piezoelectricity.....	14
2.2. Piezoelectric driver .....	15
2.3. Parameters.....	17
Frequency response.....	17
Directivity.....	18
Resonance frequency.....	18
Electric admittance .....	20
3. Researched information .....	21
Based on acoustic diaphragms .....	21
Based on silicone buffer layer .....	22
4. The loudspeaker.....	23
5. Acoustic and electroacoustic measurements .....	26
5.1. Acoustic characterisation.....	26
5.1.1. Layout.....	26
5.1.2. Results.....	27
5.2. Electroacoustic characterisation.....	40
5.2.1. Layout.....	40
5.2.2. Results.....	40
6. Laser measurements.....	42
6.1. Layout.....	42
6.2. Results .....	43
7. Inverse filter.....	45
7.1. Theory .....	45

7.2. Implementation .....	46
7.3. Results .....	47
8. Conclusions .....	49
8.1. Acoustic measurements .....	49
8.2. Electroacoustic measurements.....	53
8.3. Laser measurements .....	54
8.4. Inverse filter .....	58
9. References .....	59
APPENDICES .....	61
APENDIX A1: Inverse filter Matlab script .....	61

Total number of words: 6019

## List of figures

- Fig. 2.1: Piezoelectric crystal. General idea of working
- Fig. 2.2: Structure of piezoelectric crystal. Reproduced from [3]
- Fig. 2.3: Oscillation of the piezoelectric crystal when voltage is applied. Reproduced from [3]
- Fig. 2.4: Electric configurations of piezoelectric crystal. Reproduced from [<http://www.fuji-piezo.com/Bimorph.htm>]
- Fig. 2.5: Piezoelectric diaphragm and modes of vibration of the crystal. Reproduced from [5]
- Fig. 2.6: Relation between supporting method and frequency of resonance. Reproduced from [3]
- Fig. 2.7: Cavity of piezoelectric loudspeaker. Reproduced from [3]
- Fig. 2.8: Electric equivalent circuit of piezoelectric loudspeaker. Reproduced from [10]
- Fig. 3.1: Schematic view of a piezoelectric microspeaker. Reproduced from [13]
- Fig. 4.1: Piezoelectric tweeter. Front view
- Fig. 4.2: Piezoelectric tweeter. Back view
- Fig. 4.3: Detailed front view of piezoelectric diaphragm
- Fig. 4.4: Detailed back view of piezoelectric diaphragm
- Fig. 5.1: Brüel & Kjær 4189-L-001 microphone
- Fig. 5.2: View of the speaker in the infinite baffle and the microphone at 1 meter distance
- Fig. 5.3: a) (up) Complete loudspeaker configuration. b) (down) Measured frequency response
- Fig. 5.4: a) Naked loudspeaker configuration. b) Measured frequency response
- Fig. 5.5: Directivity of complete loudspeaker
- Fig. 5.6: Directivity of naked loudspeaker
- Fig. 5.7: a) Front opened loudspeaker configuration. b) Measured frequency response
- Fig. 5.8: Complete loudspeaker at near-field. Measured frequency response
- Fig. 5.9: Front opened loudspeaker at near field. Measured frequency response
- Fig. 5.10: a) (up) & b) (middle) Complete loudspeaker with damping material. c) (down) Measured frequency response
- Fig. 5.11: a) Loudspeaker configuration. b) Measured frequency response
- Fig. 5.12: a) Enclosure-less loudspeaker configuration. b) Measured frequency response
- Fig. 5.13: a) Tool designed for varying enclosure size. b) Loudspeaker configuration c) Measured frequency response
- Fig. 5.14: a) Loudspeaker configuration. b) Measured frequency response
- Fig. 5.15: Naked loudspeaker, back radiation. Measured frequency response
- Fig. 5.16: a) Loudspeaker configuration. b) Measured frequency response.
- Fig. 5.17: Front opened loudspeaker with bass-reflex. Measured frequency response
- Fig. 5.18: a) & b) Detailed view of rear suspension. c) Measured frequency response
- Fig. 5.19: Last loudspeaker configuration. Measured frequency response
- Fig. 5.20: Naked loudspeaker. Measured electric admittance
- Fig. 5.21: Complete loudspeaker. Measured electric admittance
- Fig. 5.22: Naked loudspeaker with added mass. Measured electric admittance
- Fig. 5.23: Improved complete loudspeaker. Measured electric admittance
- Fig. 6.1: Laser measurements layout

Fig. 6.2: Measurement points distribution

Fig. 6.3: Average acceleration over voltage of the piezoelectric diaphragm

Fig. 6.4: Acceleration over voltage in the central point

Fig. 6.5: Acceleration in the edge: point 2

Fig. 6.6: Acceleration in the edge: point 3

Fig. 6.7: Acceleration in the edge: point 2

Fig. 6.8: Acceleration in the edge: point 24

Fig. 7.1: Sound reproduction system. Reproduced from [14]

Fig. 7.2: Pre-processing frequency response of improved loudspeaker

Fig. 7.3: Designed filter frequency response

Fig. 7.4: Designed filter impulse response

Fig. 7.5: Post-processing frequency response

Fig. 8.1: Complete loudspeaker before (up) and after (down) modifications

Fig. 8.2: Zones of the diaphragm with similar behaviour

Fig. 8.3: Frequency response (red) and acceleration of the diaphragm (blue)

Fig. 8.4: 2D plot of laser scanner at 3408Hz

Fig. 8.5: 2D plot of laser scanner at 5856Hz

Fig. 8.6: Measured frequency response, inverse filter OFF

Fig. 8.7: Measured frequency response, inverse filter ON

## 1. Introduction

A loudspeaker is a device that transforms electric signal in acoustic signal. This is a transducer that produces sound in response to an electrical audio input. The electro-acoustic transduction process is divided into two steps: an electro-mechanic transduction, which transforms the electricity in movement, and a mechanic-acoustic transduction, which transforms the movement of the diaphragm to an audible signal.

There are different kinds of loudspeakers. Focussing on the mechanic-acoustic transducer, they can be divided in cone speakers or direct radiation speakers and in horn speakers or of indirect radiation. Focussing on the electro-mechanic transducer, they can be divided into four important groups: dynamic (most popular, also known as voice coil speakers), electrostatic (based on a capacitor), electromagnetic (common in headphones) and piezoelectric.<sup>[1]</sup>

Piezoelectric devices are commonly used in sounders to generate high level warning sounds or in public address (PA) systems but there are few applications of these devices in high-fidelity audio systems. This is in spite of the interesting characteristics that these devices have, such as very low price, robustness, electrical efficiency and small size.

Current ultra-thick mobile phones, tablets, micro-computers and televisions require smaller, lighter, slimmer and better components in terms of power efficiency. Inner speakers have to meet these demands. Most of the conventional speakers are not designed to be thin, since a magnetically actuated transducer requires additional depth to enhance low-frequency sound. Since the proliferation of high-definition, better quality and the most realistic sound are demanded in all devices. This work involves an experimental and bibliographic investigation about piezoelectric loudspeakers and how to reach a better sound quality in this kind of device.

## 2. Piezoelectric loudspeaker

Piezoelectric are one of the different types of speakers that exist. Unlike dynamic loudspeakers, piezoelectric sound production is not based on a magnetic field but on a special crystal that moves when an electric field is applied.

This is a piezoelectric crystal, which has piezoelectric properties.

### 2.1. Piezoelectricity<sup>[2]</sup>

Piezoelectricity is a phenomenon presented by particular crystals which accumulate electric charge in response to applied mechanical stress, like a squeeze or a general deformation. The opposite effect is also presented, which means that a mechanical strain is internally generated by the piezoelectric crystal when an electrical field is applied (this is the basis for piezoelectric loudspeakers). Once the electric field disappears the crystal recovers its original form.

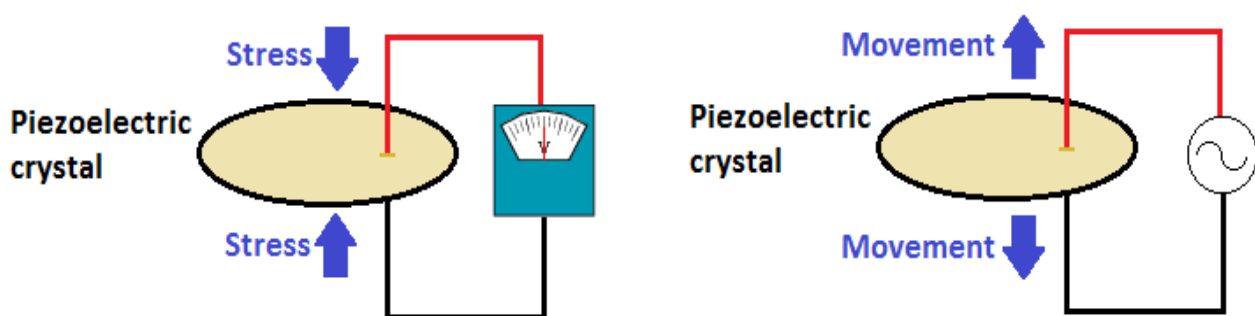


Fig. 2.1: Piezoelectric crystal. General idea of working

Piezoelectricity was discovered by the French physicists Pierre and Jaques Curies in 1881 while they were studying quartz compression. Piezoelectricity is presented in natural and synthetic crystalline materials with no inversion symmetry, which is not having a centre of symmetry.

Two big groups of piezoelectric materials can be distinguished: one group of those materials which have piezoelectric property naturally like quartz, berlinite or tourmaline, and another with the ferroelectric materials. These are synthetic materials that acquire the piezoelectric attribute after having been polarized, such as lithium tantalite ( $\text{LiTaO}_3$ ), lithium niobate ( $\text{LiNbO}_3$ ), zinc oxide ( $\text{ZnO}$ ), barium titanate ( $\text{BaTiO}_3$ ) and one of the most widely used, lead zirconate titanate, also called PZT (because of its molecular formula  $\text{Pb}[\text{Zr}_x\text{Ti}_{1-x}]\text{O}_3$ ).

## 2.2. Piezoelectric driver<sup>[3],[4],[5]</sup>

Piezoelectric crystals are used in numerous ways such as high voltage and power sources, motors, sensors, frequency standards and also actuators like loudspeakers.

The main part of the speaker is the piezoelectric diaphragm. This consists of a piezoelectric ceramic plate which has electrodes on both sides and a flexible metal plate (normally brass or stainless steel). The piezoelectric ceramic plate is attached to the metal plate with adhesives.

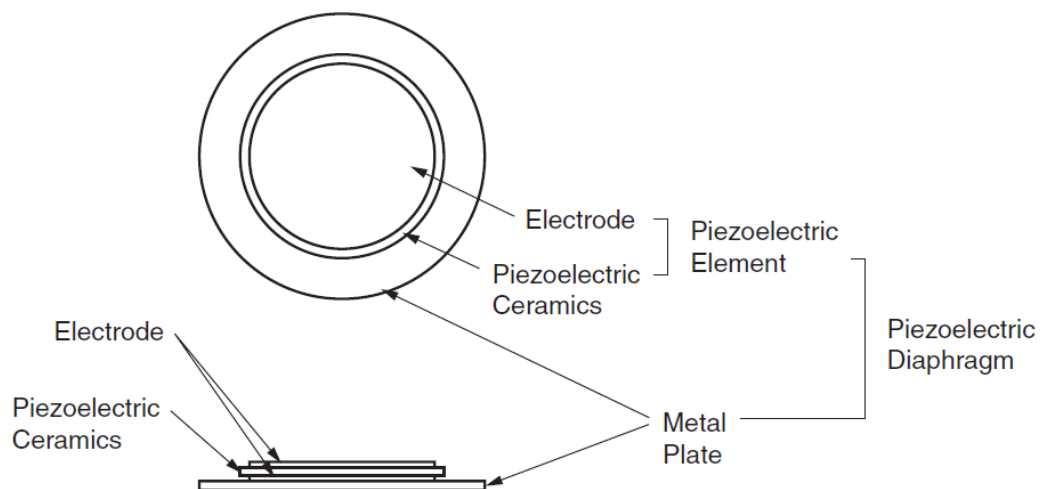
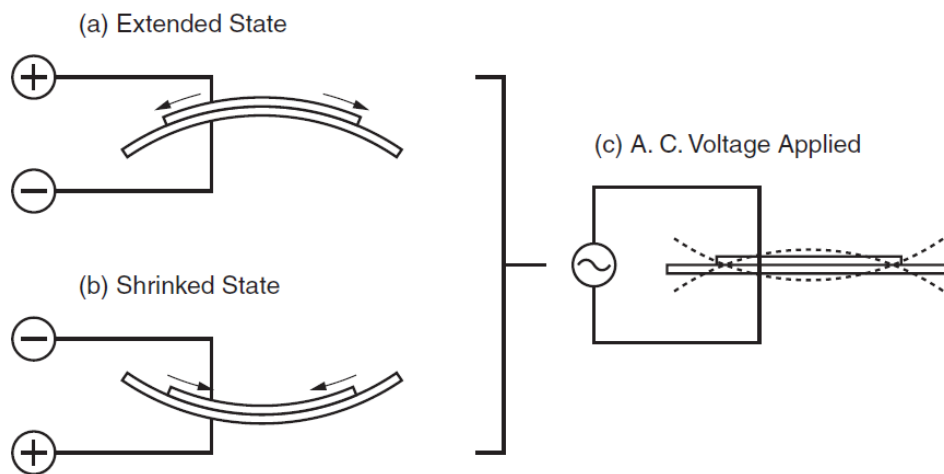


Fig. 2.2: Structure of piezoelectric crystal. Reproduced from [3]

Applying D.C. voltage between electrodes of a piezoelectric diaphragm causes mechanical distortion due to the piezoelectric effect. This can cause that the diaphragm bends as it is shown in Fig. 2.3.a). And conversely, the ceramic can shrink by applying a different voltage, bending the diaphragm on the other direction (Fig. 2.3.b). Because the ceramic is bonded to a rigid frame, the diaphragm recovers its original form when the voltage stops.



Thus, when AC voltage is applied across electrodes, the bending shown in Fig. 2.3-a and Fig. 2.3-b is repeated as shown in Fig. 2.3-c, producing sound waves in the air.



**Fig. 2.3: Oscillation of the piezoelectric crystal when voltage is applied. Reproduced from [3]**

Crystals can be monomorphic, comprised of only one crystal and bimorph, formed by two crystals with an opposite movement between the plates so that one expands and the other shrinks.

The electric configuration can be series or parallel. Next image shows the differences between bimorph series and parallel types.

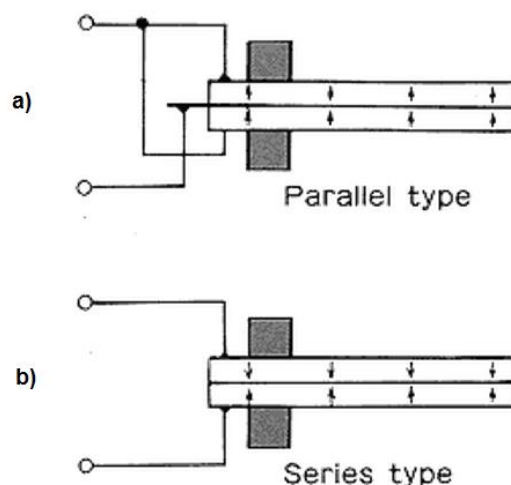


**Fig. 2.4: Electric configurations of piezoelectric crystal. Reproduced from [<http://www.fuji-piezo.com/Bimorph.htm>]**

Due to the high mechanical impedance of the mineral employed in the fabrication of the crystals, the frequency response of these devices is restricted to the high range. It is because of the rigid frame attached to the mineral and its weight why

the crystal does not have the fundamental resonance frequency out of the audible range (20 – 20 kHz).

Horn tweeter is the most widely used piezoelectric speaker. It consists of a circular disc attached to a cone which radiates sound through a plastic horn. The cone is typically made from lightweight, stiff materials such as coated paper, plastic resin film. As it is shown in the next figure, the cone is attached to the centre of the membrane since it is the point where the displacement is maximum.

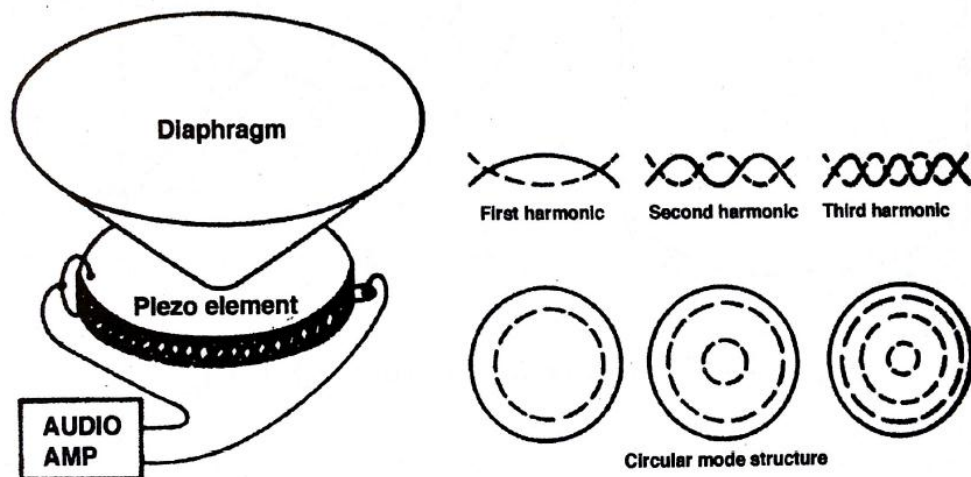


Fig. 2.5: Piezoelectric diaphragm and modes of vibration of the crystal. Reproduced from [5]

This is the configuration of the loudspeaker employed in the experimental part of the project.

### 2.3. Parameters

As it has been said in the introduction, the main aim of this work has been to research different ways of getting better a piezoelectric loudspeaker. The attempts were focussed in specific acoustic and electroacoustic parameters.

#### Frequency response<sup>[6]</sup>

The most important and informative test measurement is that of the loudspeaker's axial frequency response. The frequency response has two components: amplitude and phase, which together completely define the linear behaviour of the system. The frequency-domain representation takes the form of transfer function  $H(f)$ . This representation shows the response to an excitation signal of the loudspeaker in the full-range frequency or in a specific bandwidth.

There are several techniques for measuring the frequency-response of a loudspeaker. They can be grouped focussing on the type of the test signal employed. One of the most effective techniques uses a random noise, such as “white noise”, which contains all frequencies in a random (Gaussian) distribution, i.e. equal energy per Hz. This will show us the amplitude response of the loudspeaker in the frequency-spectrum.

### **Directivity**

Directivity is the relationship between the sound pressure in a particular angle and the maximum sound pressure which corresponds to the central axis of the loudspeaker. Polar diagram is the most common representation of directivity. It varies as a function of the frequency which must be specified on the diagram.<sup>[5]</sup> In horn speakers directivity is highly dependent on horn design.

### **Resonance frequency** <sup>[3],[7],[8]</sup>

Acoustic resonance is the tendency of an acoustic system to radiate or absorb more energy when it is forced or driven at a frequency that matches one of its own natural frequencies of vibration (its resonance frequency) than it does at other frequencies.

Resonance frequency of a speaker is the point at which the weight of the moving parts of the speaker becomes balanced with the force of the speaker suspension when in motion. The mass of the moving parts and the stiffness of the suspension of the diaphragm are the key elements that affect the resonance frequency.

In piezoelectric speakers the resonance frequency depends on the method used to support the piezoelectric diaphragm. Colombero and Sosa (2012) set the equations for calculating this frequency:

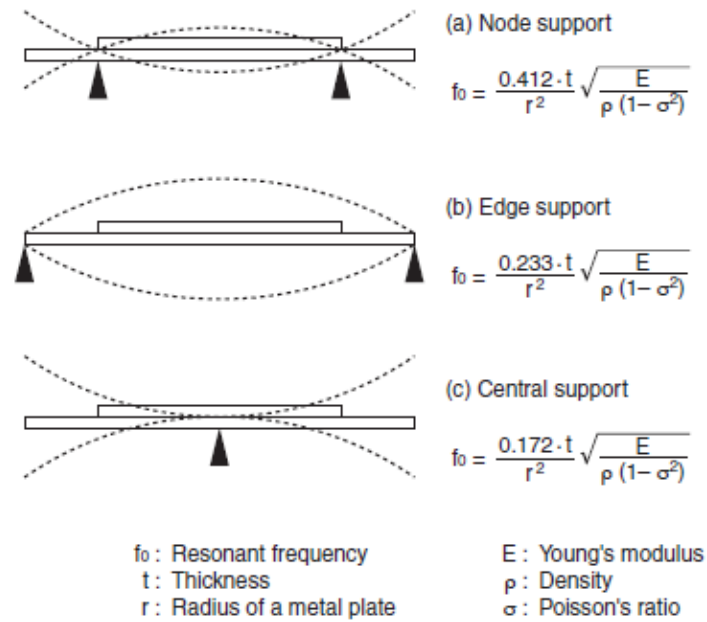


Fig. 2.6: Relation between supporting method and frequency of resonance. Reproduced from [3]

If piezoelectric diaphragm is the same in all configurations, the lowest resonance frequency corresponds with the configuration c.

Furthermore, it is important to bear in mind the resonance frequency of the enclosure (cavity) since it can reinforce a specific frequency and produce audible modifications in the output sound signal. This frequency ( $f_{cav}$ ) is obtained from Helmholtz's Formula:

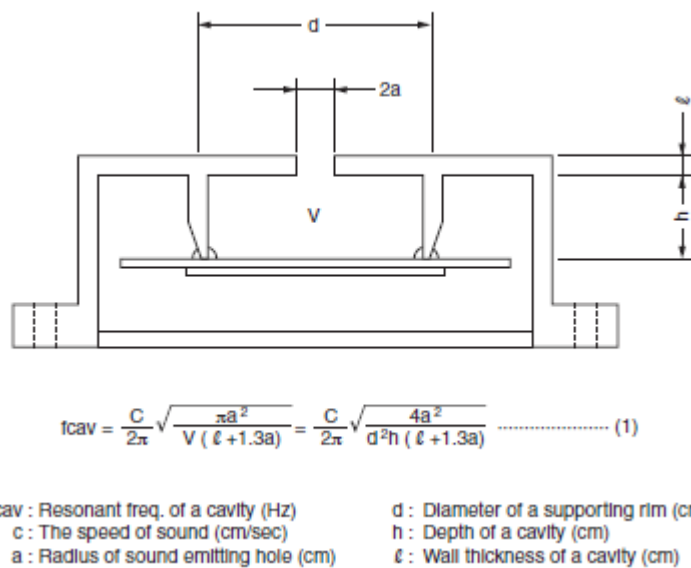


Fig. 2.7: Cavity of piezoelectric loudspeaker. Reproduced form [3]

## Electric admittance

Admittance is defined as the inverse of impedance. The electro-mechanic resonance frequency of the crystal – which is the mechanic resonance but considering the electric effect over the speaker – can be calculated by measuring the electric admittance.<sup>[7]</sup>

Piezoelectric ceramic element changes dimensions cyclically, at the cycling frequency of the field. The frequency at which the ceramic element vibrates most readily, and most efficiently converts the electrical energy input into mechanical energy is the electro-mechanic resonance frequency. Thus, this is placed where the electric admittance reach its first maximum (minimum electric impedance).<sup>[9]</sup>

The equivalent electric circuit of the tweeter is:

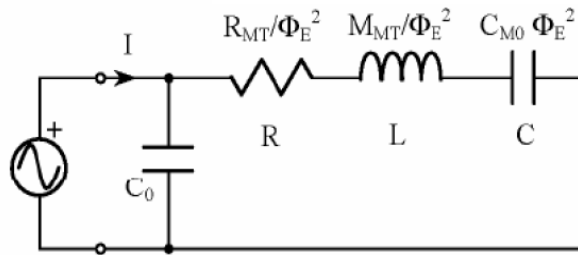


Fig. 2.8: Electric equivalent circuit of piezoelectric loudspeaker. Reproduced from [10]

It can be proved that the electro-mechanic resonance frequency of the tweeter can be calculated with the relation below <sup>[11]</sup>:

$$\omega_{0em} = \frac{1}{\sqrt{M_{mt}C_{m0}}} = \frac{1}{\sqrt{LC}} \quad (2.1)$$

Looking at the equation (2.1), it is observed that electro-mechanic resonance frequency can be decreased by adding some weight to the diaphragm.

### 3. Researched information

In this section two previous research works regarding to improve the specifications of piezoelectric loudspeakers are explained. The knowledge gained was crucial to understand the behaviour of these devices and to know what changes have more effect on the output sound signal. Some of the conclusions reached by investigators were checked in this project (measures section).

Both of them are focussed on enhancing the output in low frequency range by lowering the resonance frequency and also on getting a higher sound pressure level.

#### Based on acoustic diaphragms

Hye Jin Kim *et al.* (September 2012) investigated the vibrational characteristics of three types of acoustics diaphragms: rubber single-layer, resin film single-layer and a rubber/resin bi-layer. They concluded that the best response is given by the rubber/resin bi-layer fabricated diaphragm because the material purposed is more flexible and softer than the others which reduces its fundamental resonance frequency.

They demonstrated that the fundamental resonance frequency of a rectangular vibrating membrane is proportional to the square root of the Young's modulus and thickness of the membrane:

$$\omega_{m,n} = \sqrt{\frac{Ed}{\rho R} \left[ \left( \frac{m\pi}{a} \right)^2 + \left( \frac{n\pi}{b} \right)^2 \right]} \quad (3.1)$$

where  $E$  is the Young's modulus,  $d$  is the distance from the neutral axis to the surface of membrane,  $R$  is the radius of the curvature of the membrane at its

neutral axis,  $\rho$  is the density of the vibrating membrane,  $a$  and  $b$  are the lateral membrane dimensions, and  $m$  and  $n$  are natural numbers.

This means that to lower the fundamental resonance frequency of the piezoelectric speakers, the acoustic diaphragm must be thinner and more flexible.<sup>[12]</sup>

### Based on silicone buffer layer

Hye Jin Kim, Kunmo Koo *et al.* (December 2009) investigated the effect in the resonance frequency and in the harmonic distortion of introducing a silicone buffer layer as it is shown in Fig. 3.1.

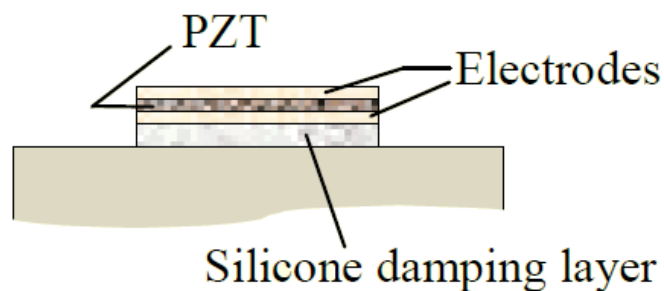


Fig. 3.1: Schematic view of a piezoelectric microspeaker. Reproduced from [13]

The results were a lower fundamental resonance frequency and hence, a wider frequency response range and a reduction of useless distortion generated by the harmonics.

Moreover, they demonstrated that the neutral axis shift due to the thick silicone buffer layer can produce more mechanical stress in the surfaces of the membrane and helps to obtain a large deflection of the diaphragm. This is based on the theory which relates stress  $\sigma(y)$  in the membrane proportionally to the strain  $\epsilon(y)$  and the normal strain linearly with the distance  $y$  from the neutral axis.<sup>[13]</sup>

## **4. The loudspeaker**

A particular piezoelectric loudspeaker was used to perform the modifications and check the theoretical knowledge. The speaker corresponds to a cheap piezoelectric tweeter. Its price is around 3 pounds, which allowed the author to experiment with several of them. Also, the low budget necessary for continuing the investigations opens new possibilities for future works and even the interest of some company.

As it is showed in the next images the tweeter is formed by a lightweight coated paper cone attached to a piezoelectric crystal which radiates sound through a plastic horn.

The piezoelectric diaphragm consists of a circular, bimorph crystal of 23 mm in diameter with two crystals vibrating with opposite movement and two electrodes. After breaking one of the ceramic crystals it could be observed that it has a parallel electric configuration, as shown in figure 2.4-a above.

As it can be seen in Fig. 4.3, a coated paper cone is glued to the crystal and finally the whole diaphragm is lightly fixed to the plastic structure in two opposite points by the wires of the electrodes (Fig. 4.4).





Fig. 4.1: Piezoelectric tweeter. Front view



Fig. 4.2: Piezoelectric tweeter. Back view



Fig. 4.3: Detailed front view of piezoelectric diaphragm

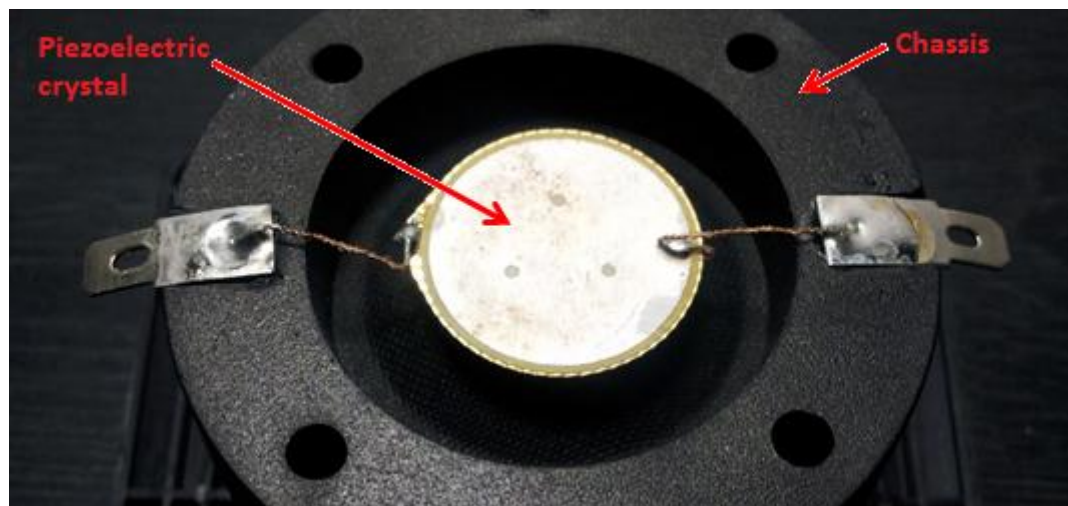


Fig. 4.4: Detailed back view of piezoelectric diaphragm

## 5. Acoustic and electroacoustic measurements

The measuring process was divided into two main parts. The first part was carried out in the small anechoic chamber at ISVR, where acoustic and electroacoustic characterisations were performed in both original state and modified loudspeaker. The modifications were decided after a literature research process and the experience gained in the previous research papers in section 3.

### 5.1. Acoustic characterisation

#### 5.1.1. Layout<sup>[10]</sup>

Measurements were taken in the small anechoic chamber of the ISVR where free-field conditions are reproduced over 180Hz, a frequency low enough for the response of the tweeter under review. As measuring platform PULSE analyser 3560C by Brüel & Kjær was used. The pre-amplified microphone utilized was the model 4189-L-001 by Brüel & Kjær. Its sensitivity is 50mV/Pa and the frequency range goes from 6.3 Hz to 20 kHz. A stereo amplifier, SA-230 by Monacor was also needed



Fig. 5.1: Brüel & Kjær 4189-L-001 microphone

As it is shown in the Fig. 5.2 the speaker was introduced in an infinite baffle providing minimal 'air spring' restoring force to the cone. This minimizes the change in the driver's resonance frequency caused by the enclosure. The microphone was placed at 1m from the central point of the speaker and the speaker was excited with random noise from 20Hz to 25,6KHz.

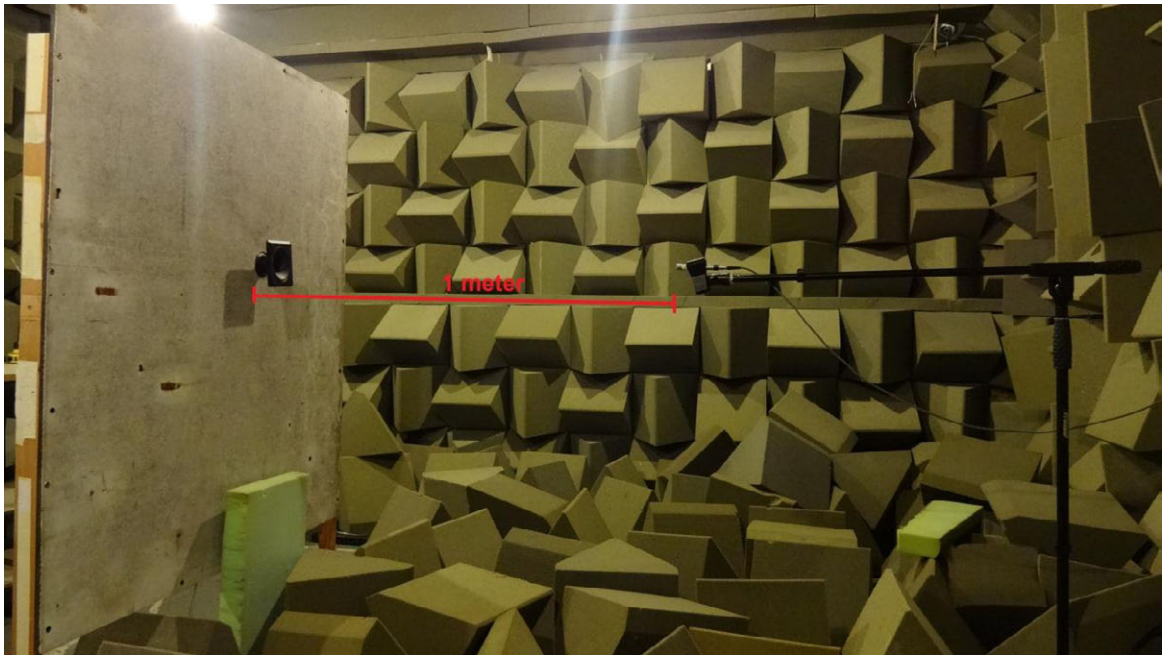


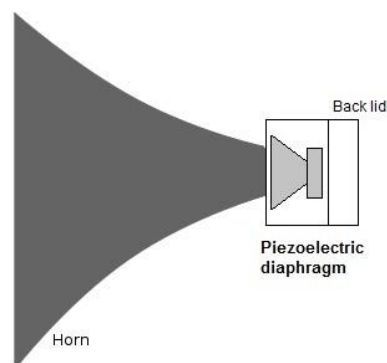
Fig. 5.2: View of the speaker in the infinite baffle and the microphone at 1 meter distance

### 5.1.2. Results

Loudspeaker was acoustically characterised by measuring the frequency response, first in the original conditions and also after every change that was introduced to it. The modifications affected to the membrane and the enclosure. The measurements were taken both attaching the horn and with the naked tweeter. Additionally, directivity was calculated for the original driver. Sixty measures were performed, here are plotted only the most relevant measurements that are useful to draw conclusions.

#### ***Complete loudspeaker***

*Complete* situation corresponds to the tweeter in selling disposition (with back lid and horn).



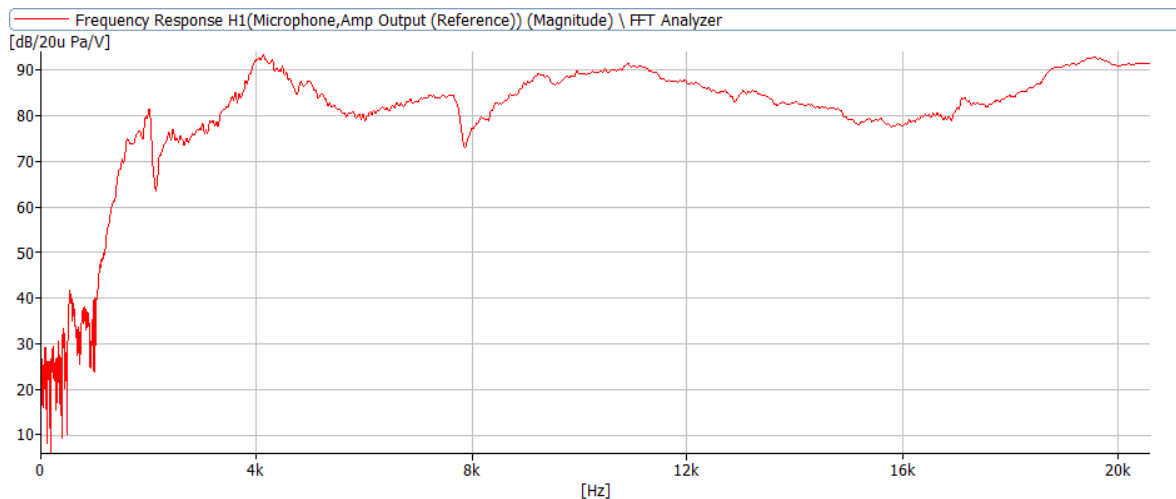


Fig. 5.3: a) (up) Complete loudspeaker configuration. b) (down) Measured frequency response

### ***Naked loudspeaker***

*Naked* situation corresponds to removing both horn and back lid from the tweeter.

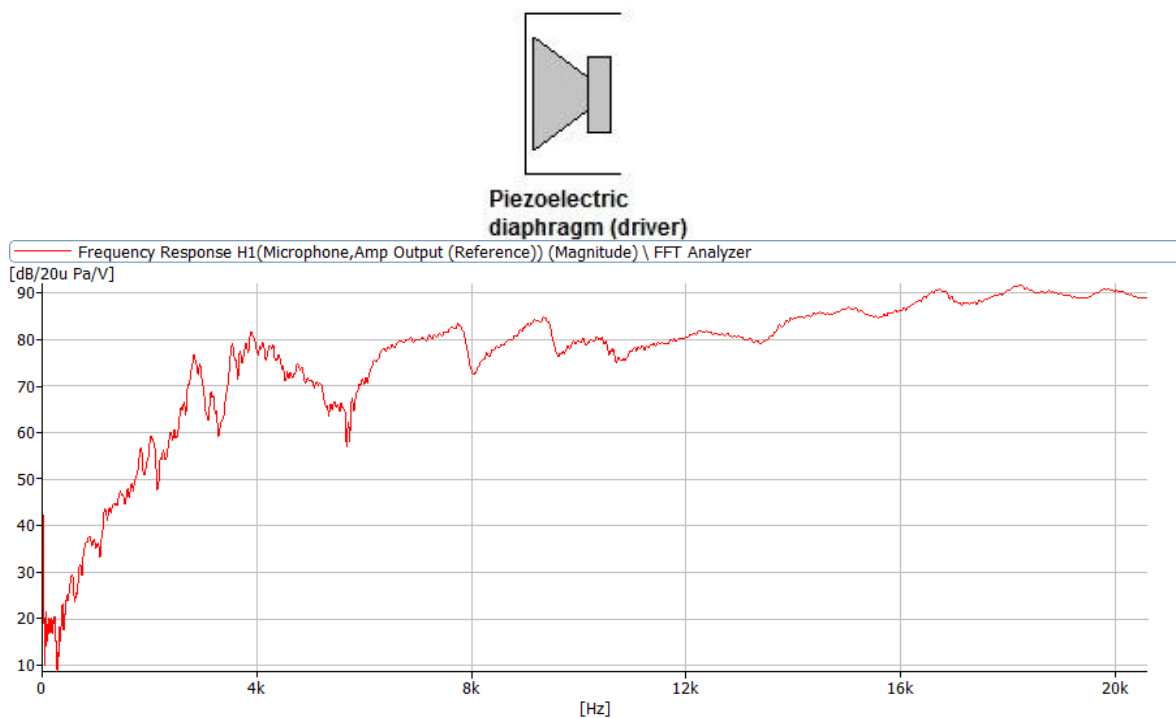
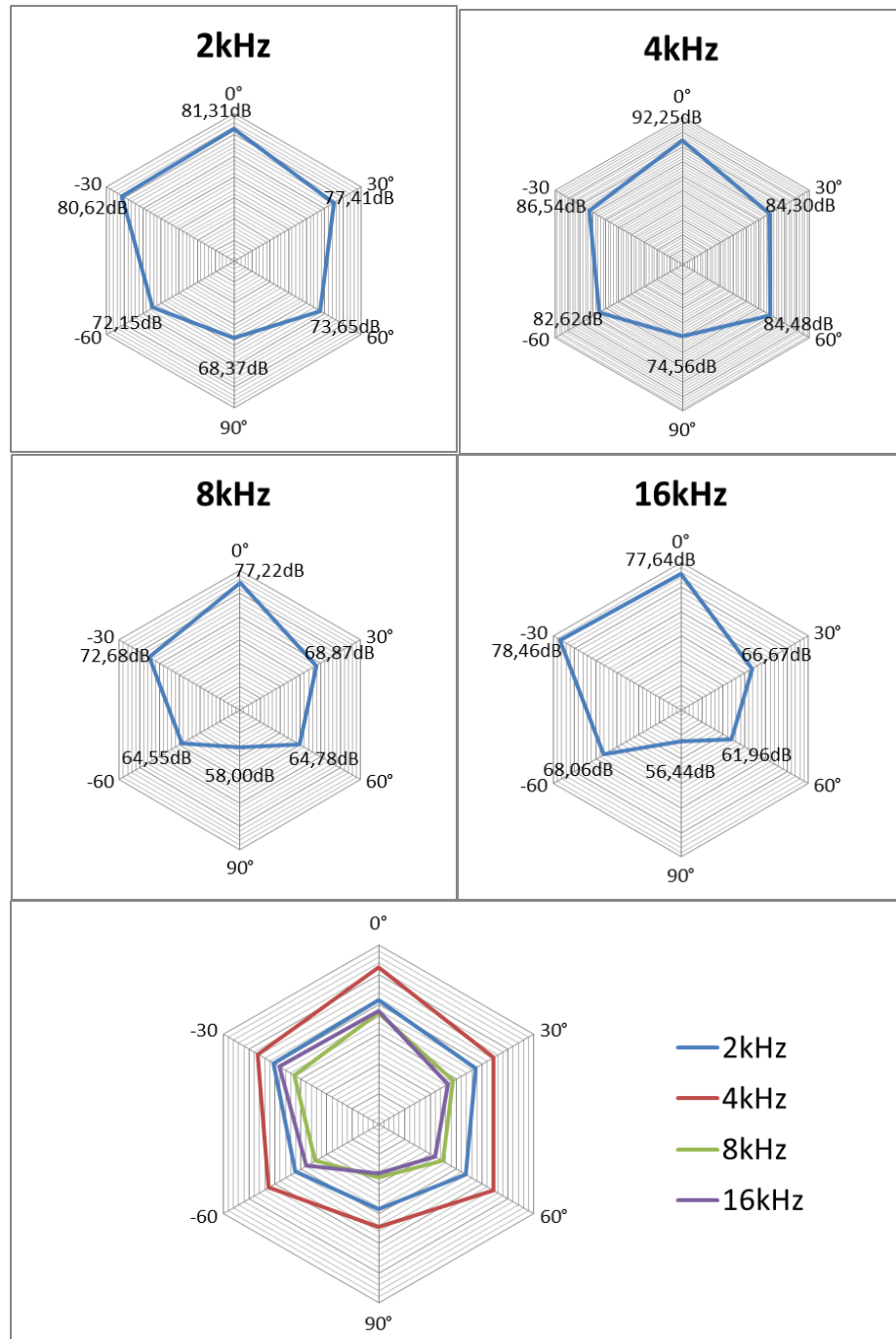


Fig. 5.4: a) Naked loudspeaker configuration. b) Measured frequency response



### ***Directivity, complete loudspeaker***

Directivity at 2kHz, 4kHz, 8kHz and 16kHz was calculated by measuring the frequency response when the loudspeaker was angled 0,  $\pm 30$ ,  $\pm 60$  and  $\pm 90$  degrees with respect to the microphone.



**Fig. 5.5: Directivity of complete loudspeaker**

## Directivity, naked loudspeaker

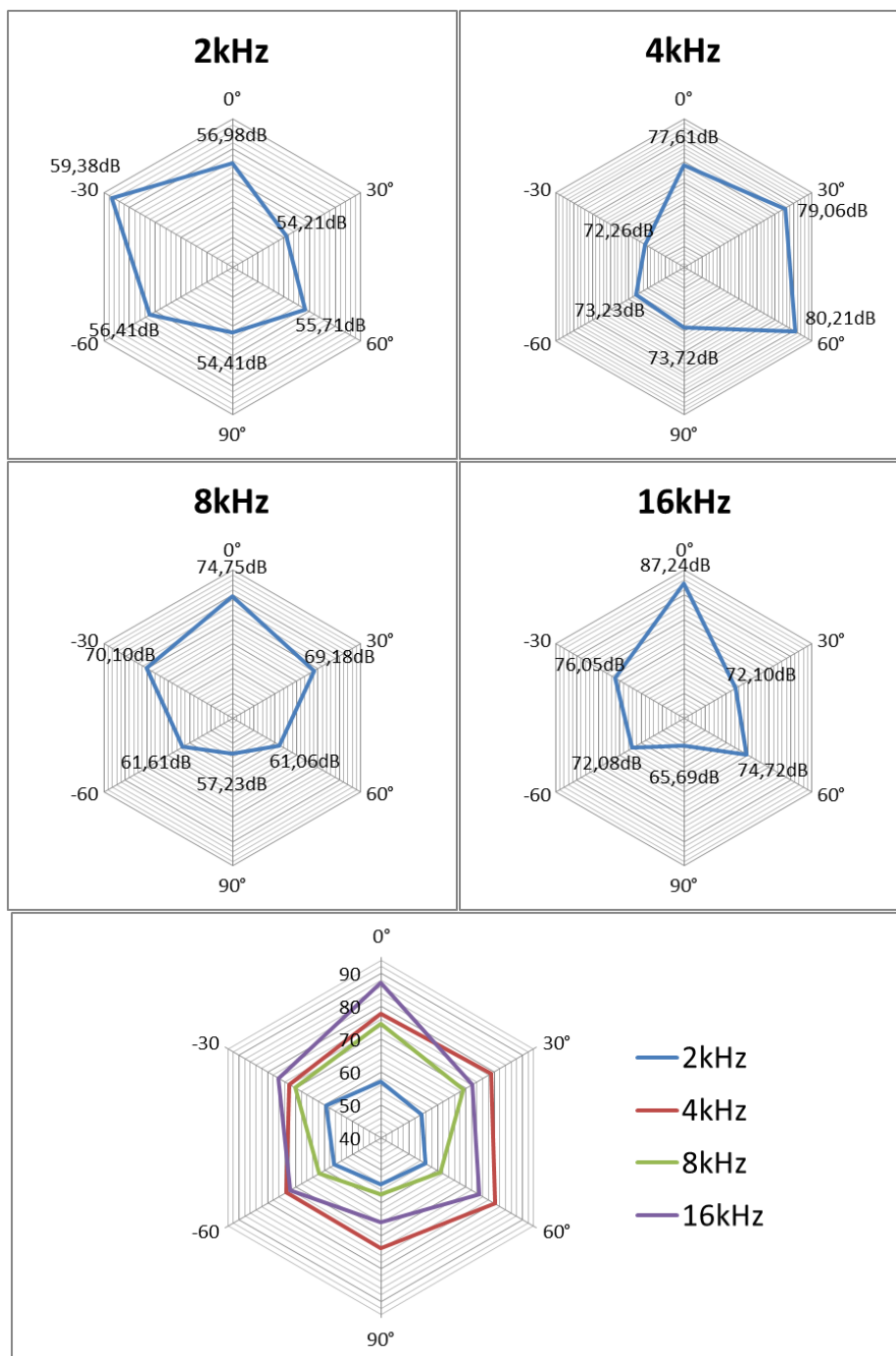
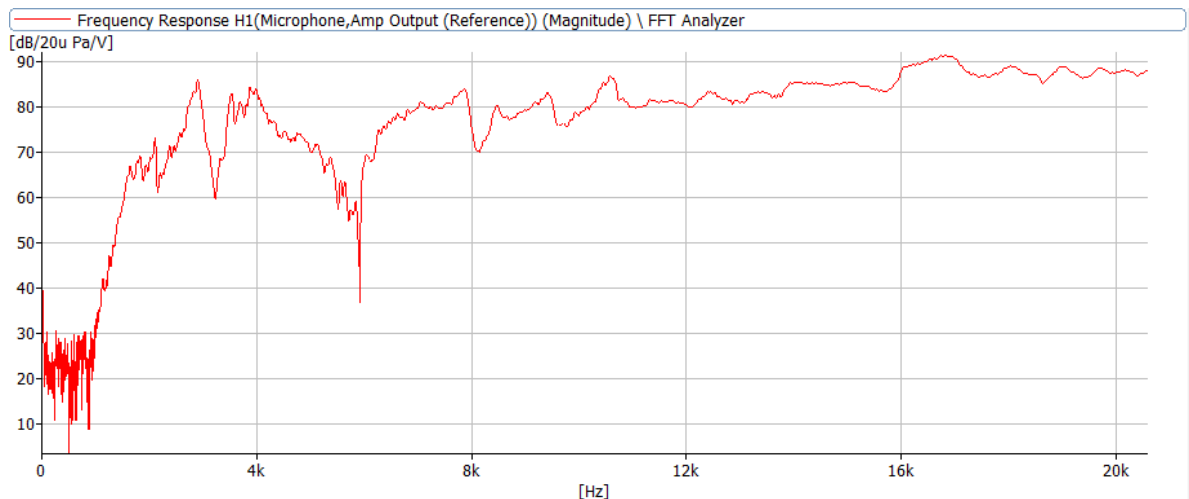
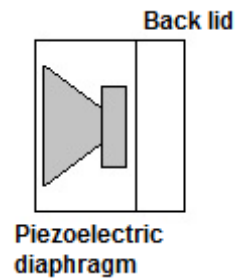


Fig. 5.6: Directivity of naked loudspeaker

### ***Front opened loudspeaker***

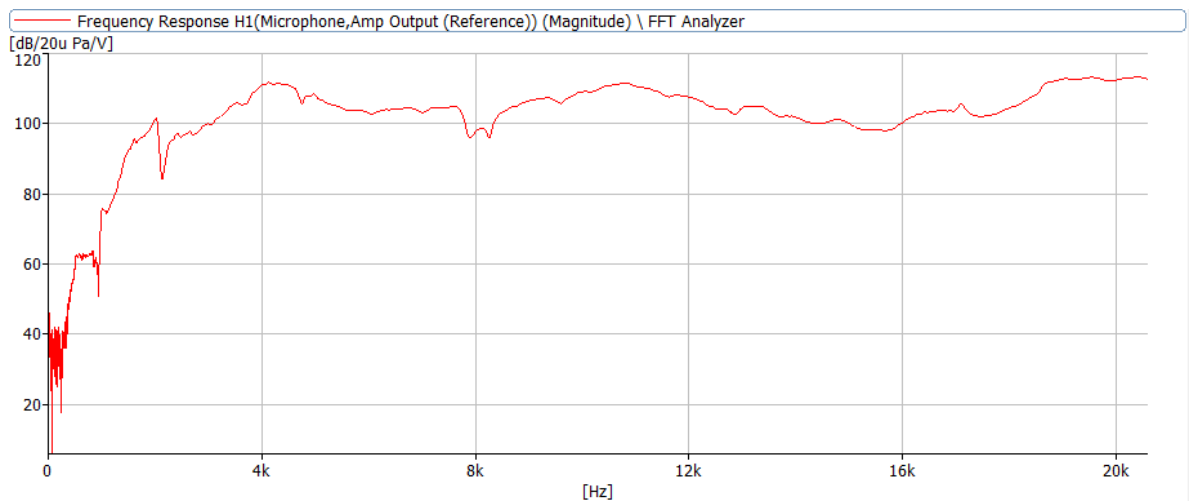
*Front open* situation corresponds to only the horn removed from the tweeter.



**Fig. 5.7: a) Front opened loudspeaker configuration. b) Measured frequency response**

### ***Complete loudspeaker at near-field***

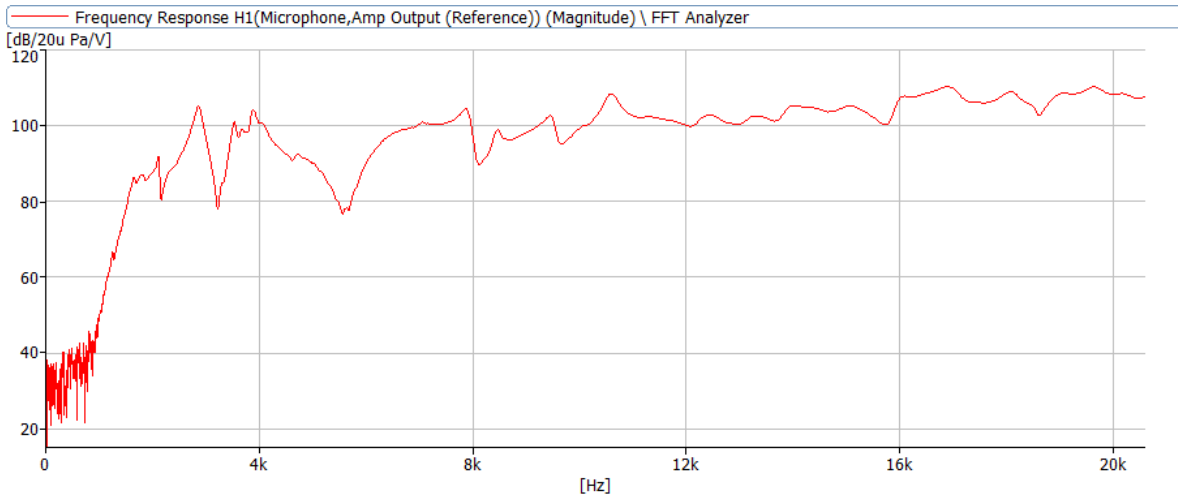
*Near field* means measuring at 10cm distance from the tweeter instead of 1m.



**Fig. 5.8: Complete loudspeaker at near-field. Measured frequency response**



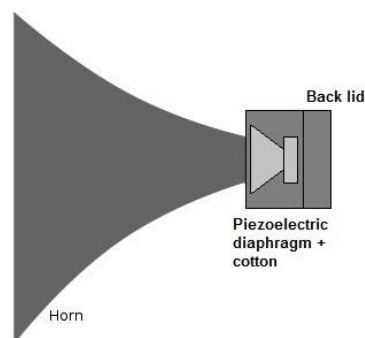
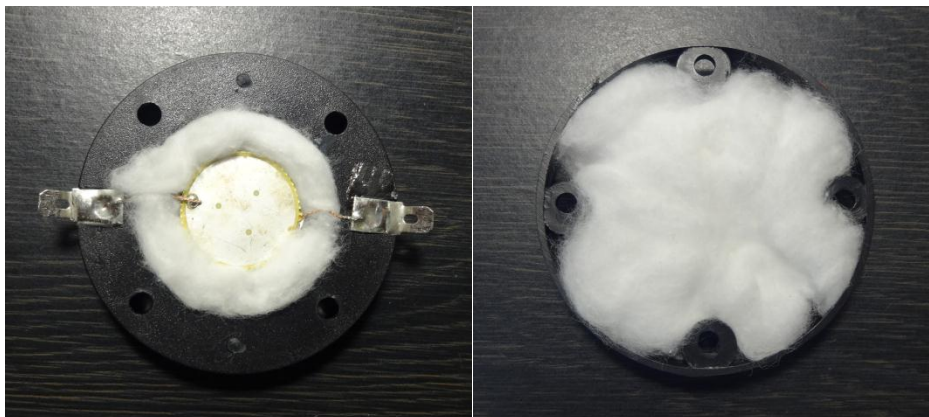
### ***Front opened loudspeaker at near field***



**Fig. 5.9: Front opened loudspeaker at near field. Measured frequency response**

### ***Complete loudspeaker introducing damping material***

The effect of introducing an absorptive material, such as cotton, inside the enclosure of the speaker was investigated. In this case, as it is shown in Fig. 5.10.a), the enclosure was filled with cotton and also with the back side of the piezoelectric diaphragm.



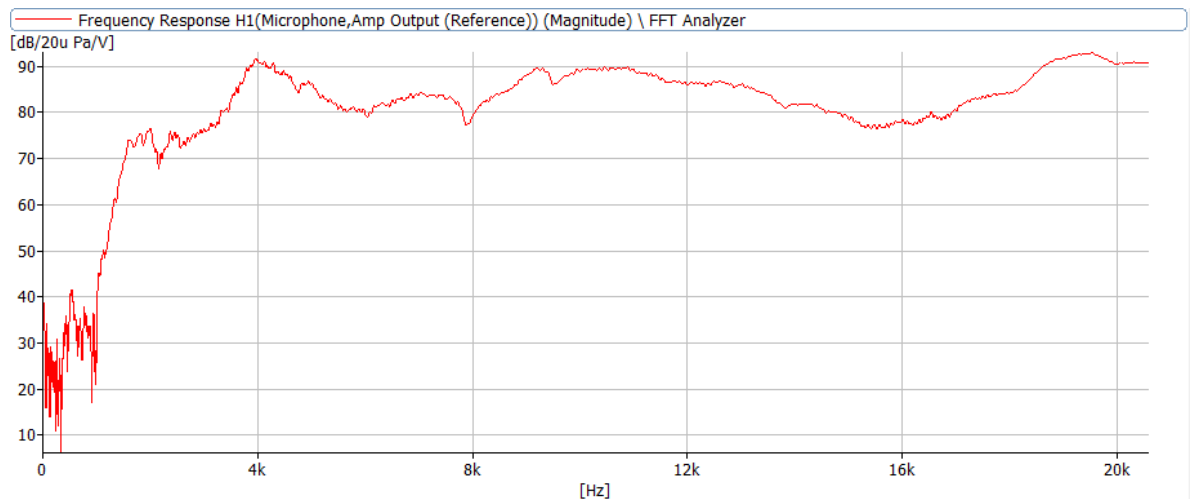
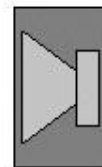


Fig. 5.10: a) (up) & b) (middle) Complete loudspeaker with damping material. c) (down) Measured frequency response

### ***Naked loudspeaker with cotton only inside the back side of the diaphragm***

In this case the cotton was only introduced in the back side of the piezoelectric diaphragm.



Piezoelectric  
diaphragm +  
cotton

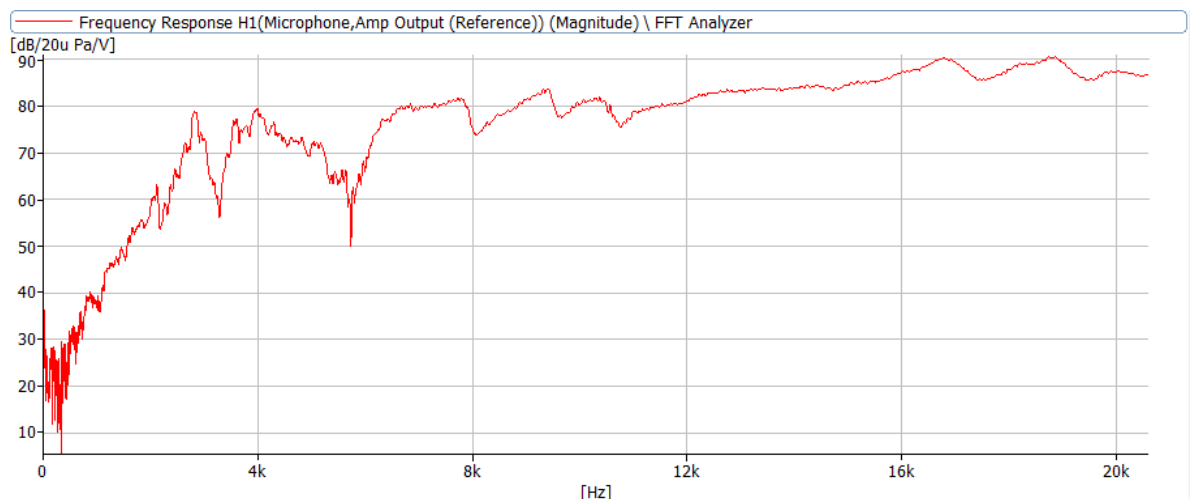
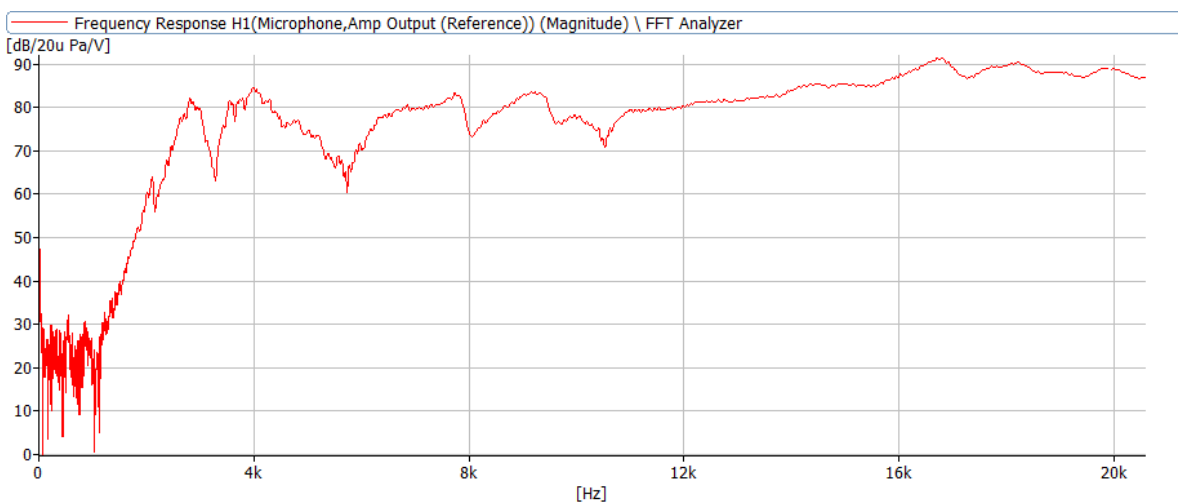
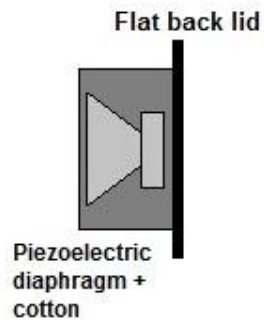


Fig. 5.11: a) Loudspeaker configuration. b) Measured frequency response

### ***Front opened loudspeaker, removing the enclosure***

In this measurement, a flat lid was attached to the back of the loudspeaker reducing the amount of air behind the diaphragm. Cotton is also present inside.



**Fig. 5.12: a) Enclosure-less loudspeaker configuration. b) Measured frequency response**

### ***Front opened loudspeaker, empty enclosure 5.5cm***

The tool shown in the Fig. 5.13.a) was designed to modify the size of the enclosure. It is made with wood and allows to make the enclosure bigger in steps of 1,5cm.

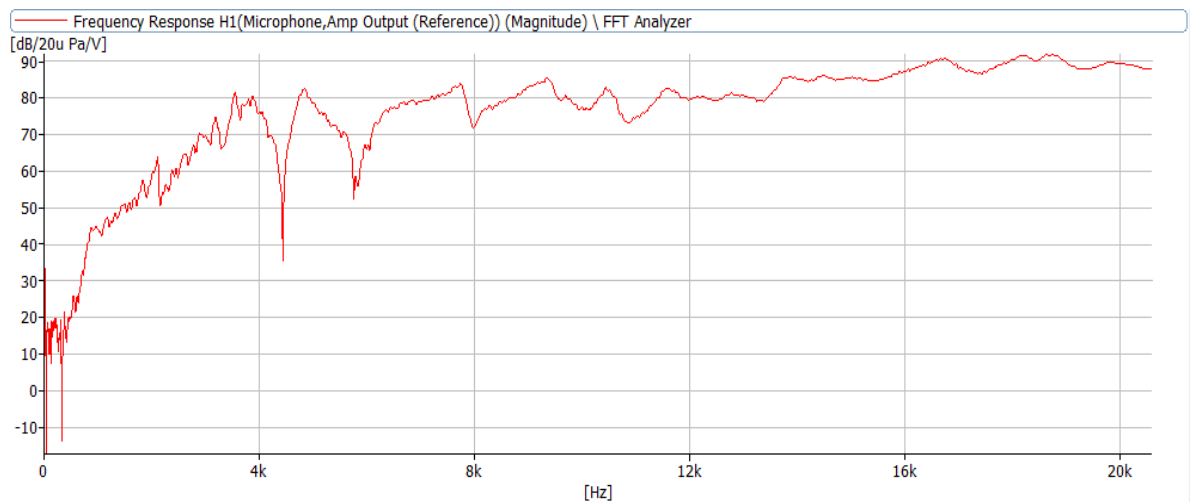
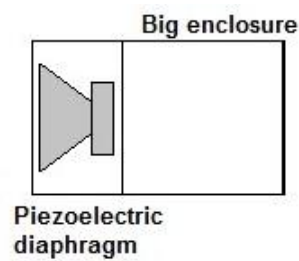
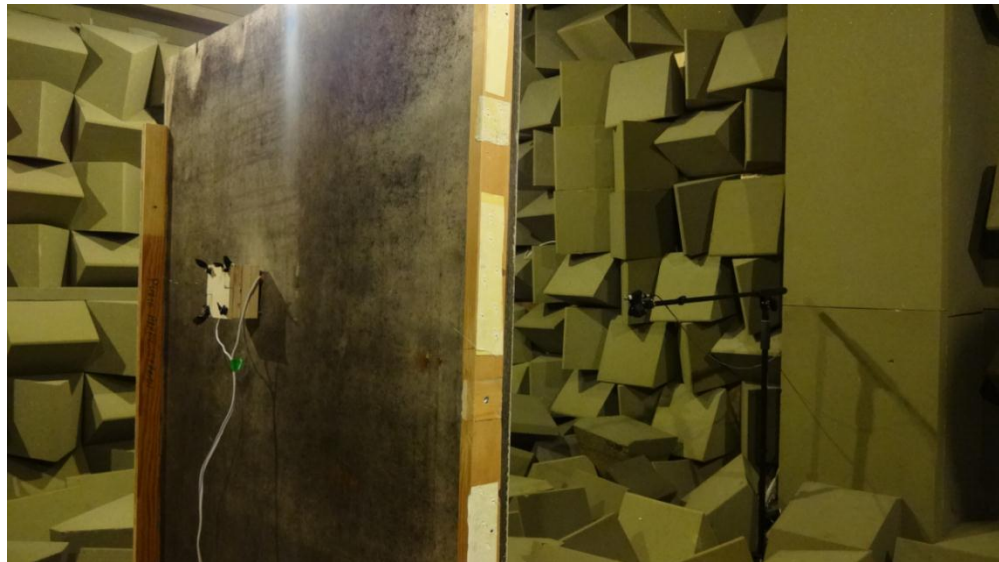


**Fig. 5.13: a) Tool designed for varying enclosure size. b) Loudspeaker configuration c) Measured frequency response**

### ***Complete loudspeaker with front air chamber***

The behaviour of the speaker when the enclosure is moved to the front of the diaphragm was measured; which means to create an air chamber between the horn and the piezoelectric membrane.

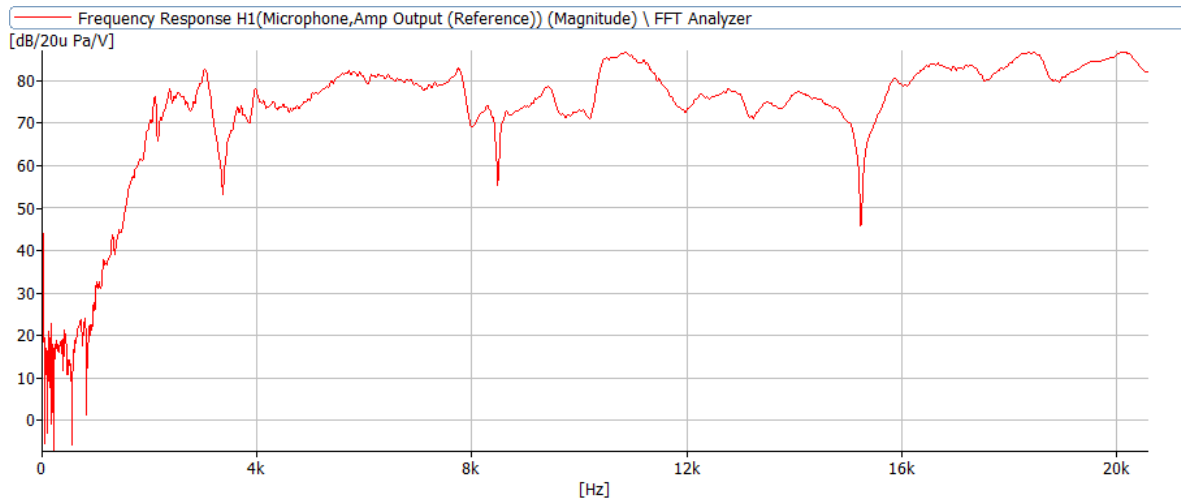
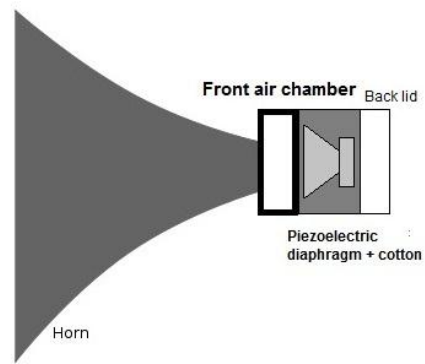


Fig. 5.14: a) Loudspeaker configuration. b) Measured frequency response

### ***Naked loudspeaker, back radiation***

The radiation from the back of the driver was measured.

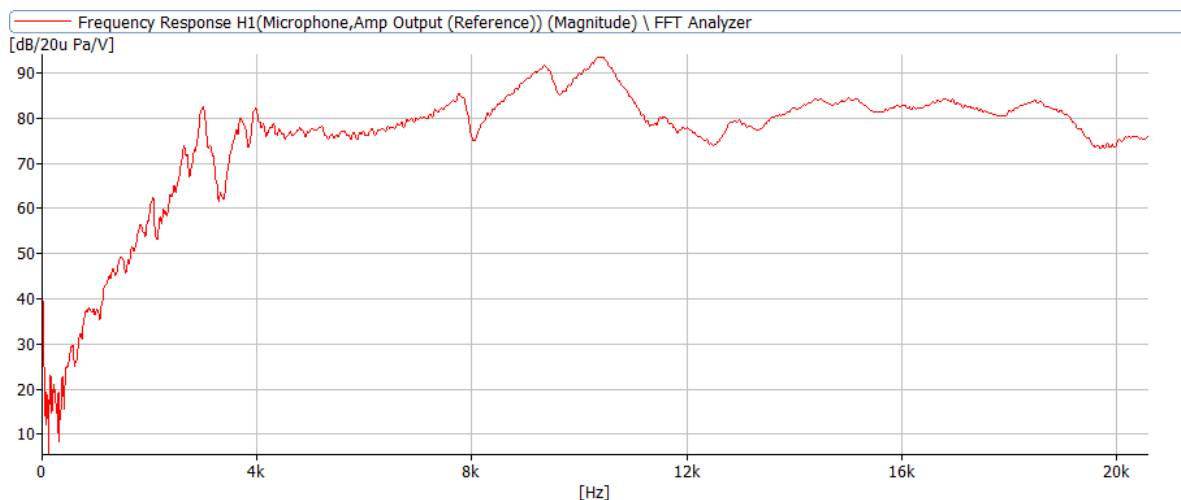


Fig. 5.15: Naked loudspeaker, back radiation. Measured frequency response

### ***Naked loudspeaker, only piezoelectric crystal***

The coated paper cone was removed from the acoustic diaphragm to see the effect of this lightweight piece attached to the crystal.

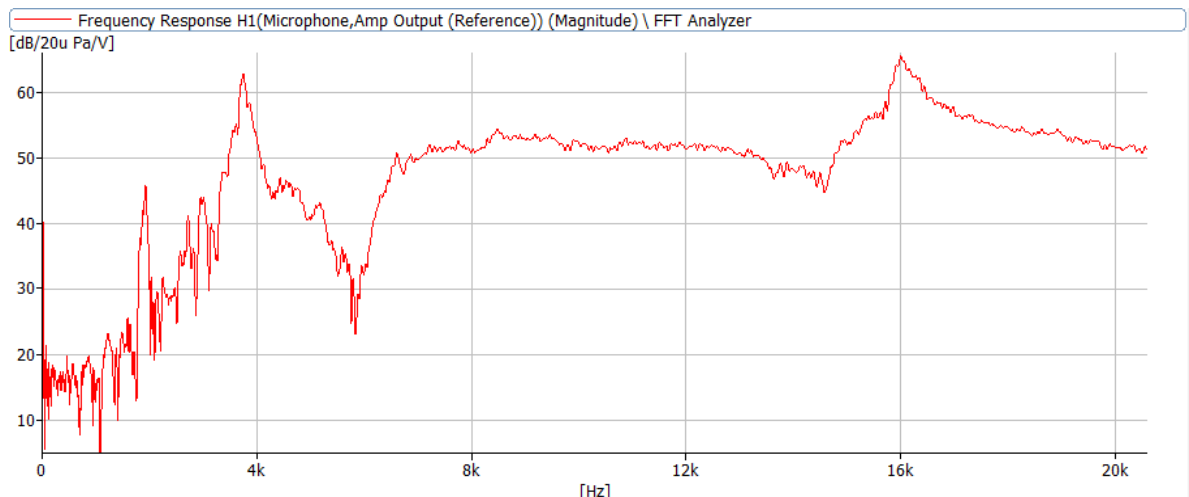
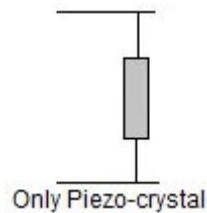


Fig. 5.16: a) Loudspeaker configuration. b) Measured frequency response.

### ***Front opened loudspeaker, bass reflex***

The effect of making a bass reflex in the enclosure of the tweeter was investigated. This is an opening in the back lid to tune the cabinet resonance to a desired frequency. In the experiment, the bass reflex consisted of a 10mm-diameter hole in the centre of the back lid.

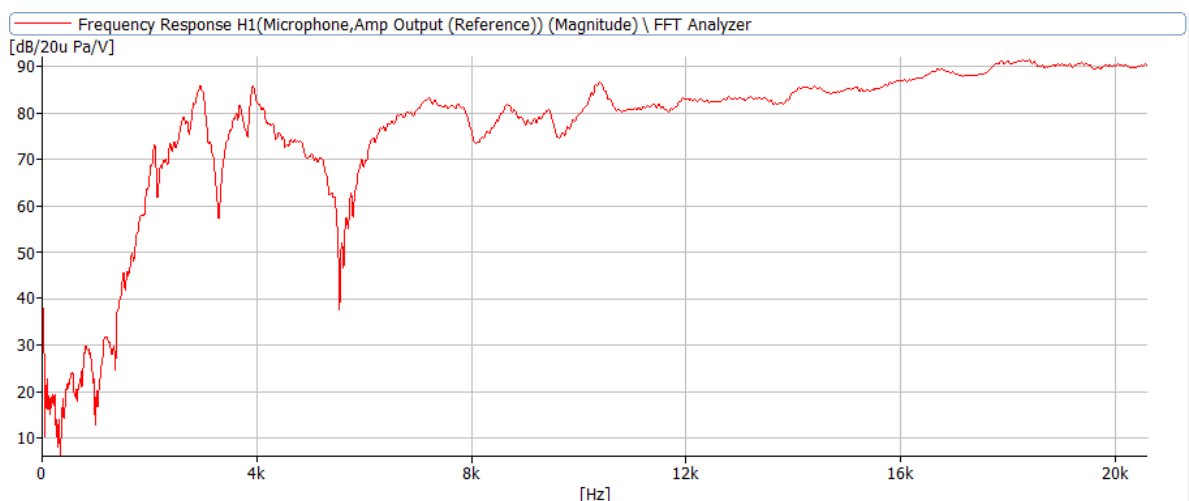
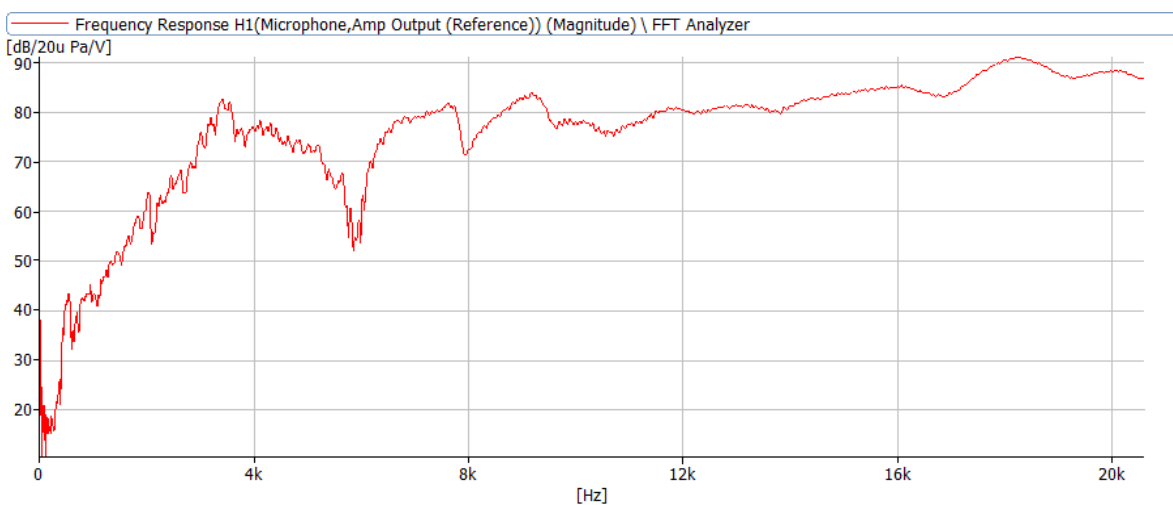
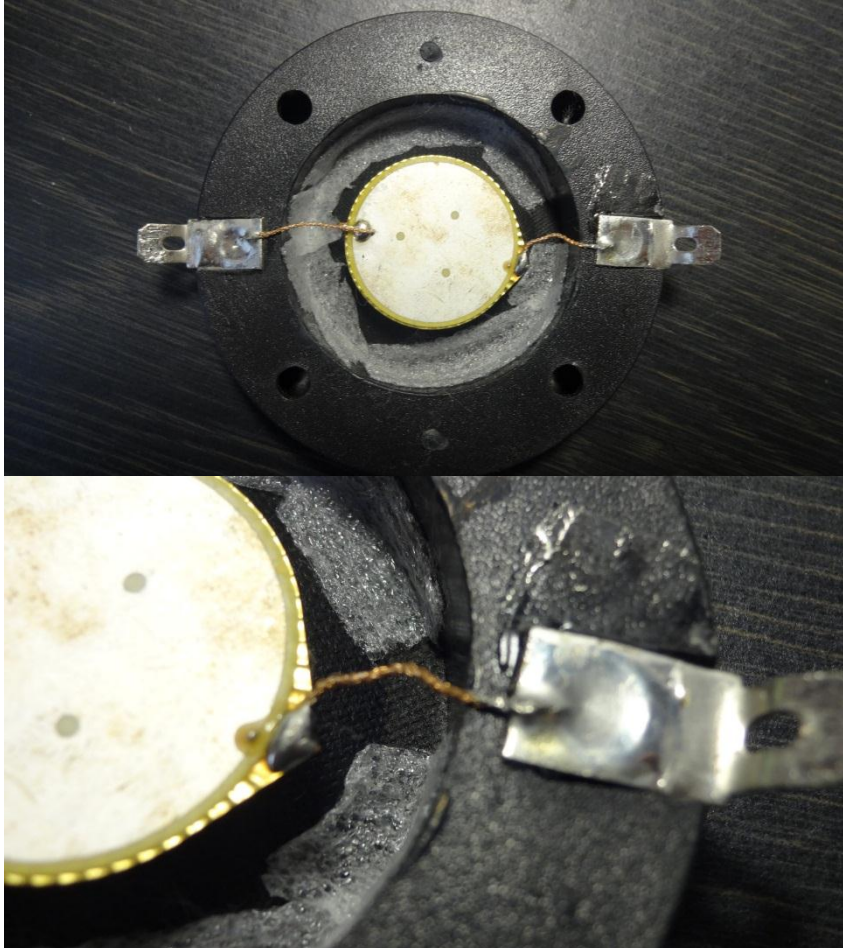


Fig. 5.17: Front opened loudspeaker with bass-reflex. Measured frequency response

### ***Naked loudspeaker with rear suspension***

The last configuration investigated the effect of providing the loudspeaker with a rear suspension to guide the vibration of the piezoelectric diaphragm. To this end, a flexible material was glued in the back side of the driver so that, as it is shown in the Fig. 5.18.a & b, the coated paper is not only glued to crystal but also to the plastic structure (chassis). This avoids crystal vibrates horizontally.



**Fig. 5.18: a) & b) Detailed view of rear suspension. c) Measured frequency response**

### ***Complete loudspeaker with rear suspension***

Finally, the complete loudspeaker with the rear suspension was measured.

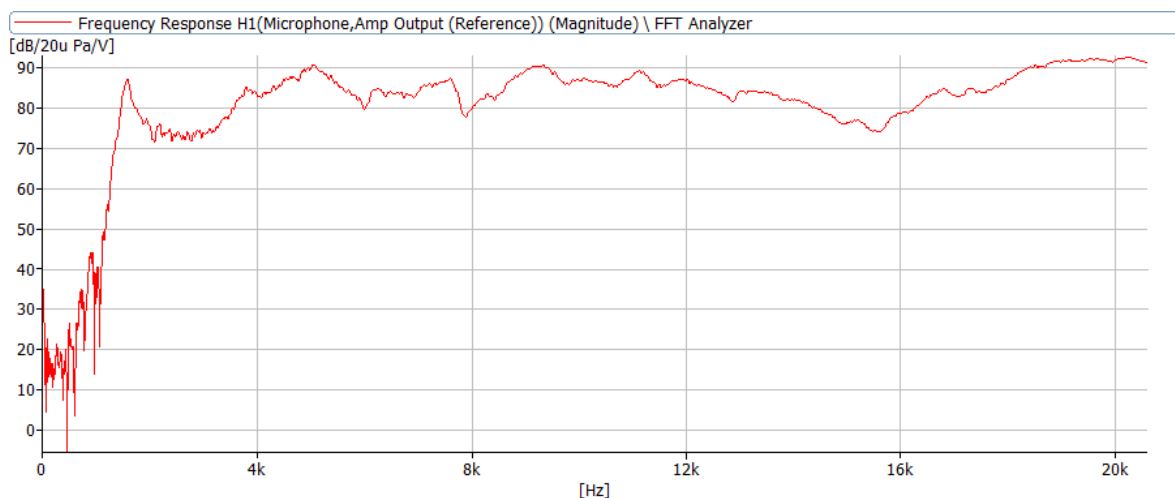


**Fig. 5.19: Last loudspeaker configuration. Measured frequency response**



## 5.2. Electroacoustic characterisation

### 5.2.1. Layout<sup>[10]</sup>

Electro-mechanic resonance frequency was calculated through the electric admittance measurement. This was performed with Pulse platform. The tweeter was excited with random noise and it was set to constant voltage by using a series 1 Ohm resistance.

The interesting frequency is marked with a cursor and its value is denoted with x in the right side banner.

### 5.2.2. Results

#### *Naked loudspeaker*

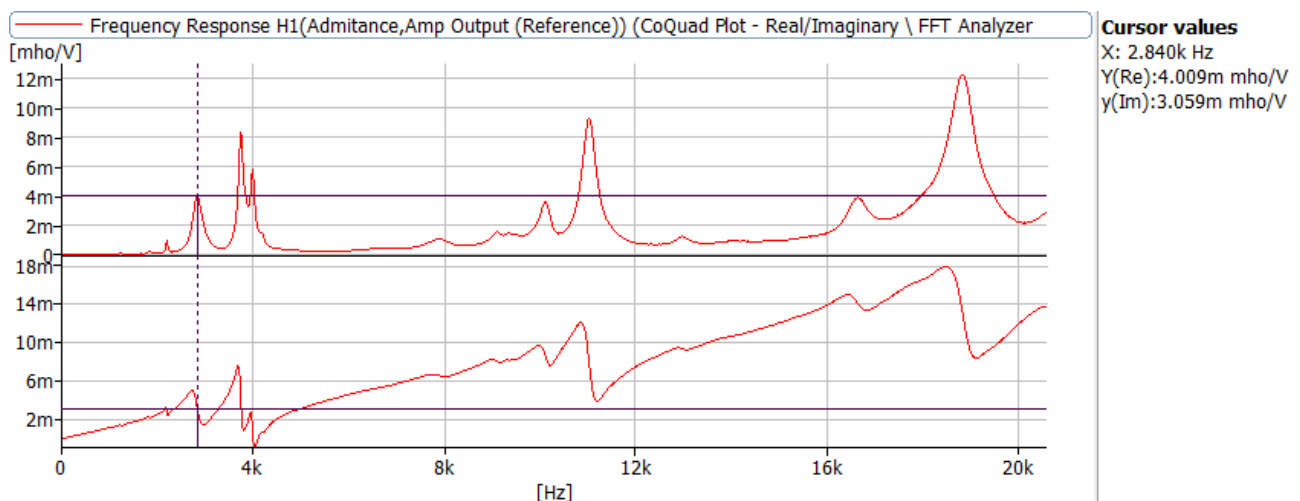


Fig. 5.20: Naked loudspeaker. Measured electric admittance

$$f_{0em} = 2840 \text{ Hz}$$

#### *Complete loudspeaker*

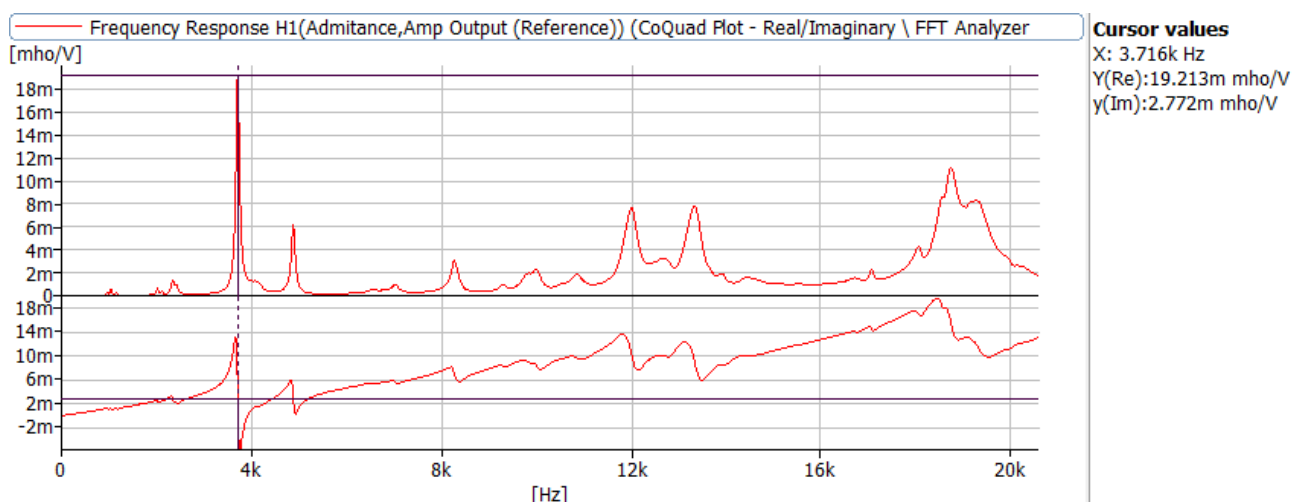
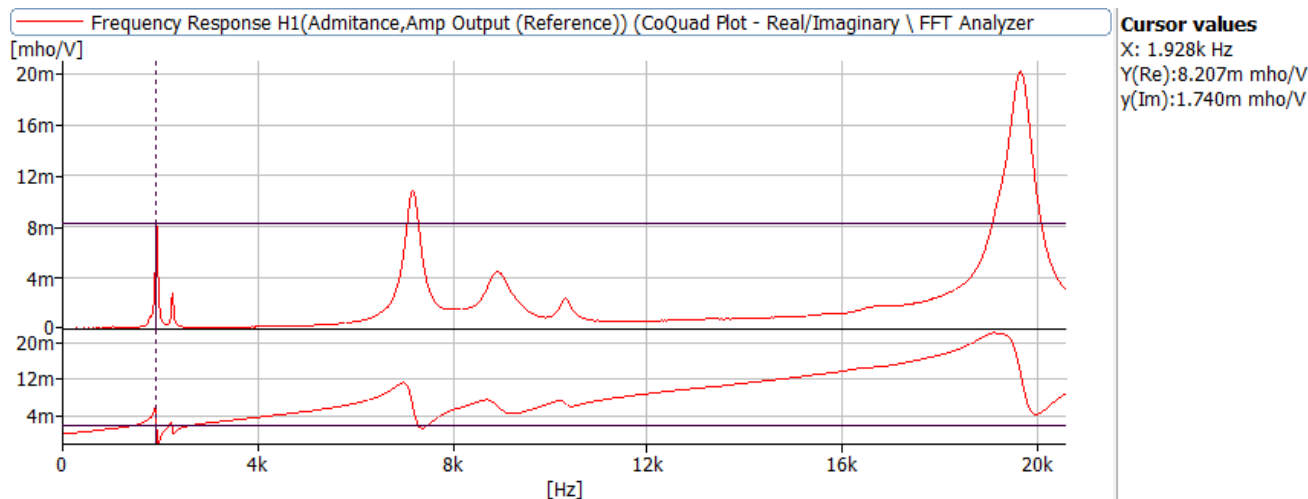


Fig. 5.21: Complete loudspeaker. Measured electric admittance

$$f_{0em}=3716\text{Hz}$$

### ***Naked loudspeaker with added mass***

A 5p coin was glued to the piezoelectric diaphragm in order to confirm the theory that inversely relates Mass of the diaphragm and resonance frequency.



**Fig. 5.22: Naked loudspeaker with added mass. Measured electric admittance**

$$f_{0em}=1928\text{Hz}$$

### ***Completed loudspeaker with rear suspension***

The resonance frequency of the most acoustically successful configuration above (Section 5.1.2, Fig. 5.19) was measured.

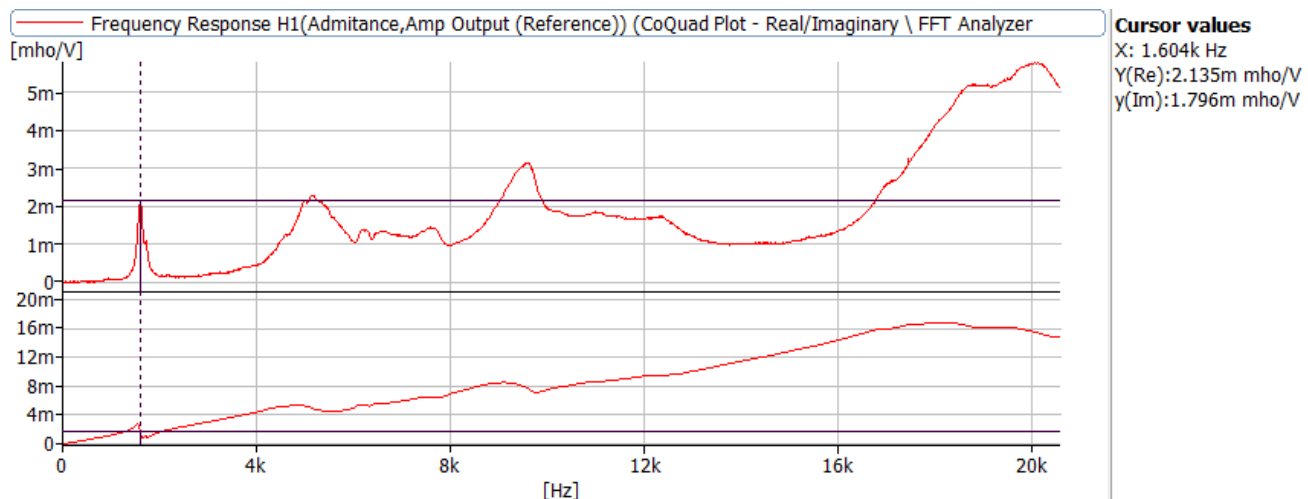


**Fig. 5.23: Improved complete loudspeaker. Measured electric admittance**

$$f_{0em}=1604\text{Hz}$$

## 6. Laser measurements

This part of the project involves a structural study of the piezoelectric diaphragm. It consists of analysing with a laser vibrometer scanning the vibration of the diaphragm to know its behaviour and also to search an explanation to the peaks and troughs remaining.

### 6.1. Layout

Laser measurements were performed in Dynamic Group Laboratory at ISVR by using a *Polytec Vibrometer Scanning Laser*.

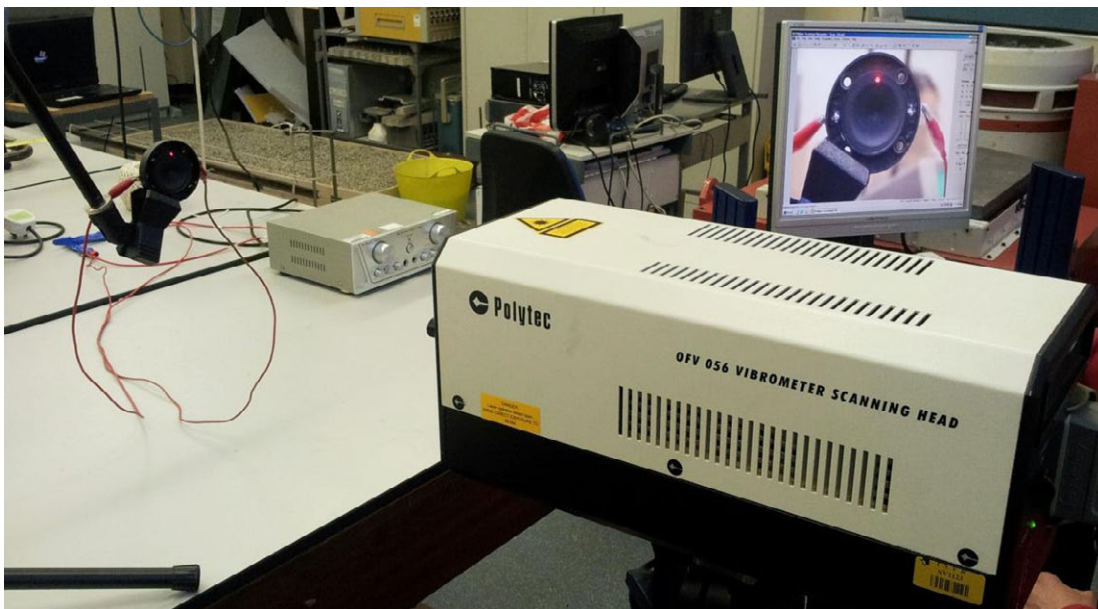


Fig. 6.1: Laser measurements layout

The laser has measured in 25 different points along the diaphragm and the average acceleration of all the points was calculate in Matlab after implementing a function to post-process the data.

## 6.2. Results

As it has been said, the scanner was performed from the vibration of 25 different points of the diaphragm. By exporting the data to Matlab it is possible to plot the acceleration at every point.

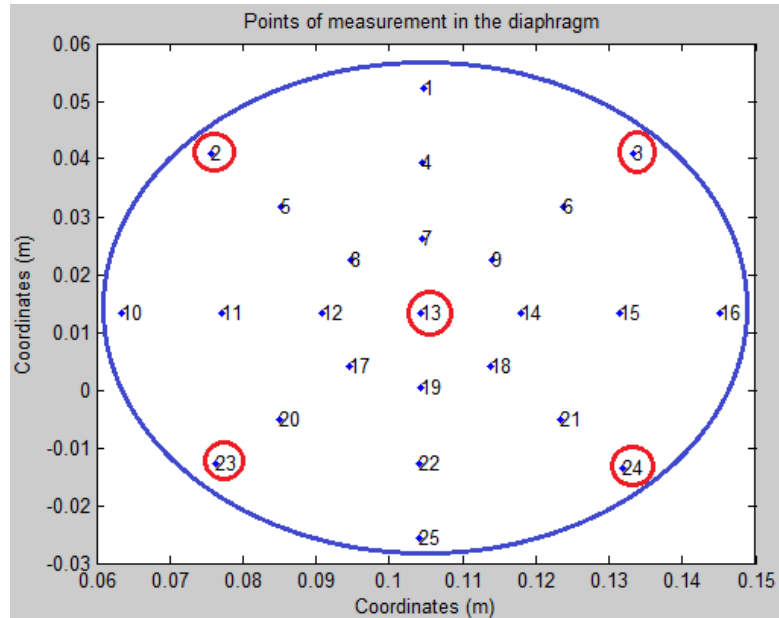


Fig. 6.2: Measurement points distribution

Next figure shows the average acceleration of the diaphragm over the input voltage calculated in Matlab. It can be seen that, as in acoustic response, some peaks and troughs are present.

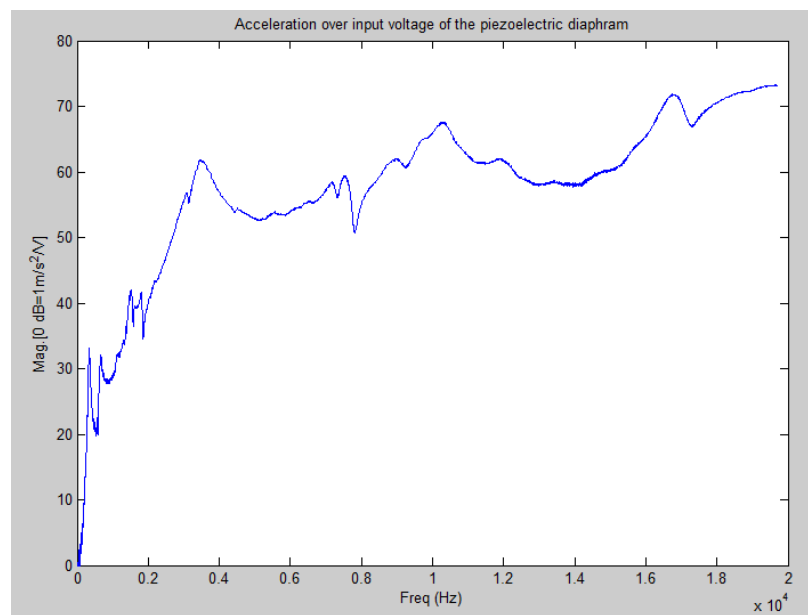
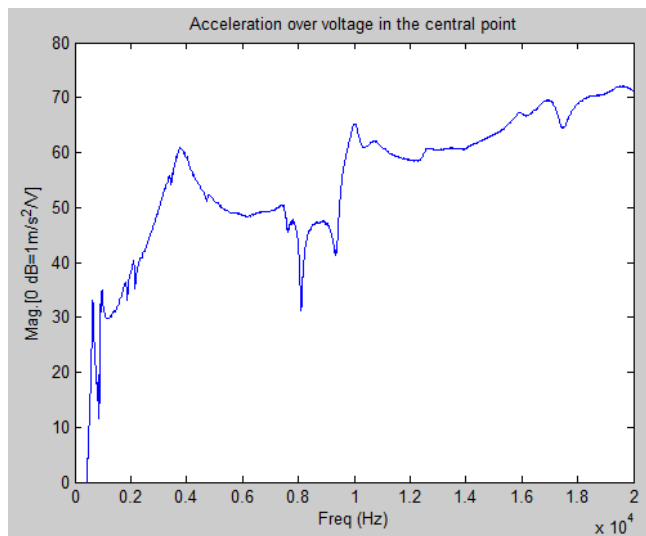


Fig. 6.3: Average acceleration over voltage of the piezoelectric diaphragm

From the exported data to Matlab it is possible to plot the acceleration at every point. Next figure illustrates the acceleration in the central point of the membrane.

This is an interesting point as this point presents the maximum of displacement at certain frequency.



**Fig. 6.4: Acceleration over voltage in the central point**

Moreover, acceleration in the points 2, 3, 23 and 24 (point symmetrically placed) is plotted to compare the vibration in the edges of the diaphragm.

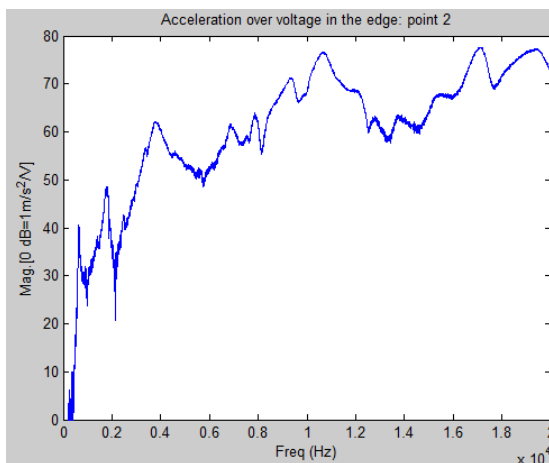


**Fig. 6.5: Acceleration in the edge: point 2**

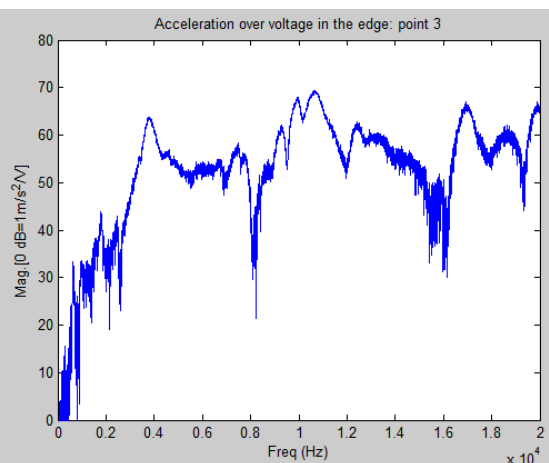


**Fig. 6.6: Acceleration in the edge: point 3**

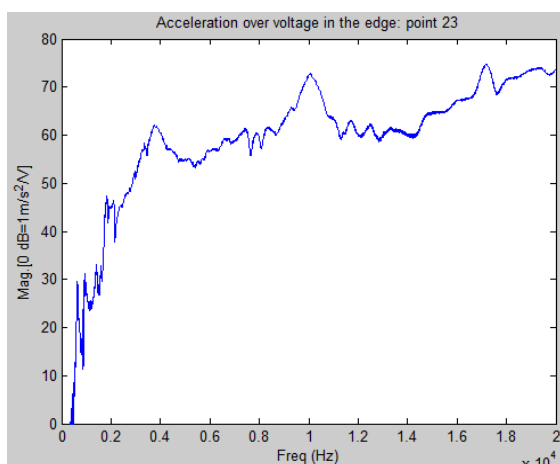


**Fig. 6.7: Acceleration in the edge: point 23**

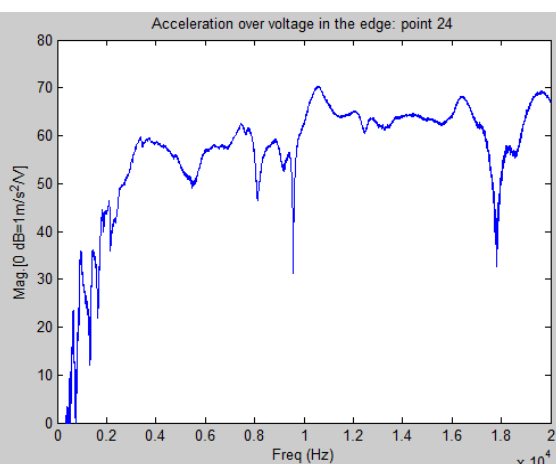


**Fig. 6.8: Acceleration in the edge: point 24**

## 7. Inverse filter

The last part of the project involved the design of a filter in order to control the input signal and obtain a flat reproduction along frequency.

### 7.1. Theory<sup>[14]</sup>

The mechanism chosen for designing the filter is based on a single channel case of the filter inversion theory developed by Ole Kirkeby *et al*, 1996 in *Local sound field reproduction using digital signal processing*. Here, researchers explain the *Least-square inversion* theory and apply it to the discrete-time multichannel sound reproduction system below.

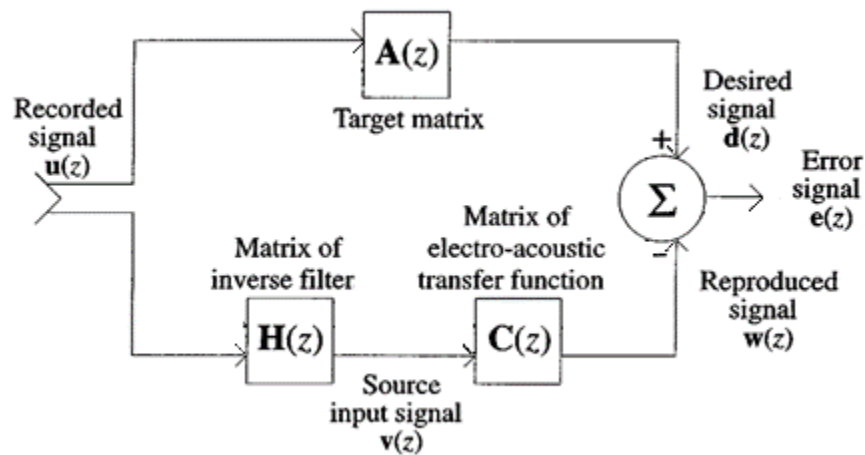


Fig. 7.1: Sound reproduction system. Reproduced from [14]

$A(z)$  is the matrix which contains the desired signal,  $C(z)$  is the matrix of transfer function and  $H(z)$  contains the coefficients of the filter that allows get  $A(z)$  by convolving it with  $C(z)$ .

For the practical case in this project,  $A(z)$  is 1, since a flat response is wanted;  $C(z)$  is the transfer function of the tweeter measured with Pulse and  $H(z)$  is the desired filter.

It can be demonstrated that the matrix of inverse filters  $H(z)$  must be chosen according to

$$H_0(e^{j\omega T_s}) = [C^H(e^{j\omega T_s}) C(e^{j\omega T_s}) + \beta I]^{-1} \cdot C^H(e^{j\omega T_s}) A(e^{j\omega T_s}) \quad (7.1)$$

The positive real  $\beta$  number is a regularization parameter that determines how much weight to assign to the „effort“ term. By varying  $\beta$  from zero to infinity, the solution changes gradually to control the amount of electrical energy used by the filter.

## 7.2. Implementation

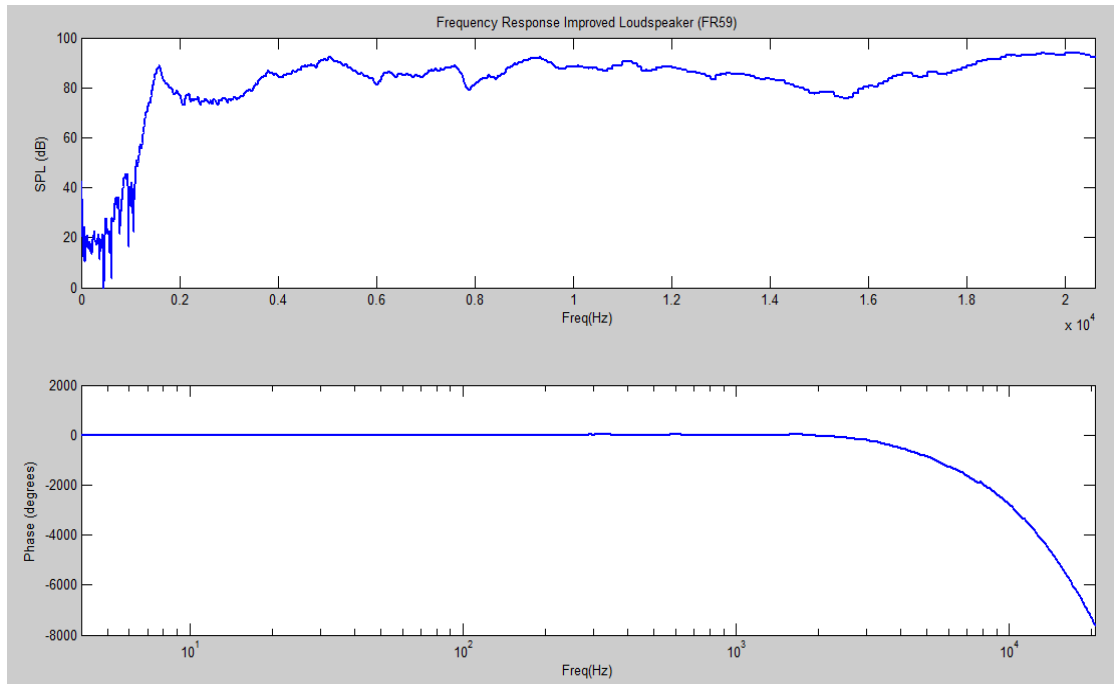
Focussing on frequency response of the acoustically improved loudspeaker (Section 5.1.2, Fig. 5.19), Matlab filter was designed to reach a flat response at the output of the tweeter.

In order to set a feasible system, signal amplification was limited to 12dB, which would mean eightfold the input voltage in some frequencies. This has been adjusted with an iterative method until a suitable  $\beta$  was found.

Code of the Matlab's script can be found in the appendix A1.

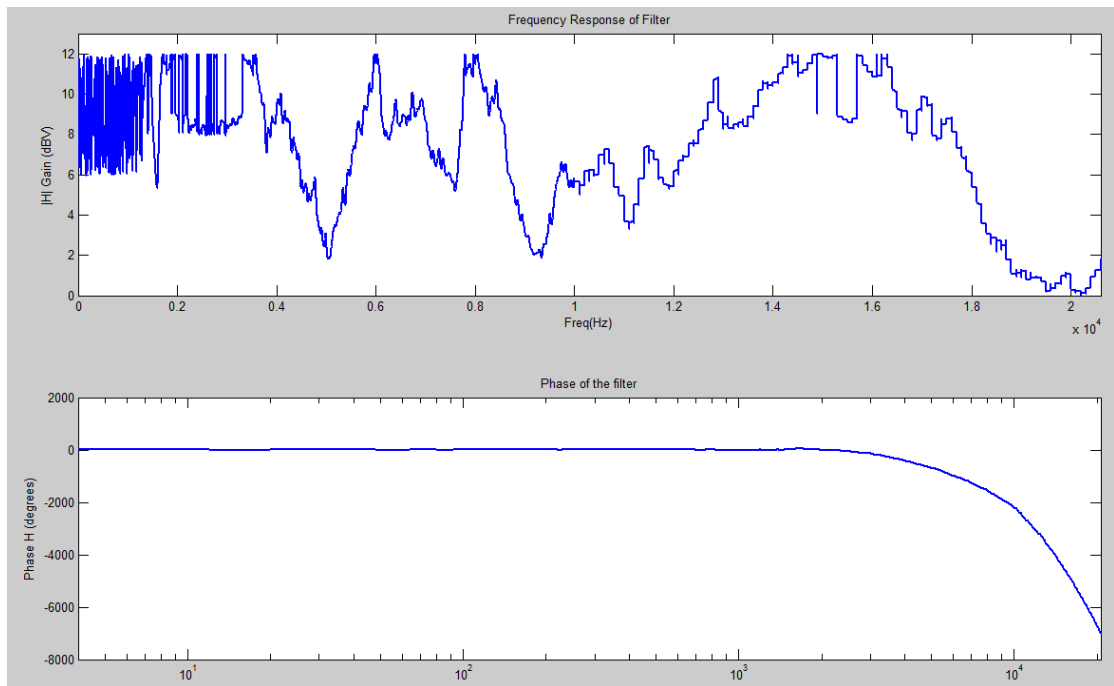
### 7.3. Results

Figure 7.2, as figure 5.19, shows the frequency response in magnitude and phase of the improved tweeter.



**Fig. 7.2: Pre-processing frequency response of improved loudspeaker**

Figure 7.3 presents the frequency response of the filter designed to improve the output of the speaker.



**Fig. 7.3: Designed filter frequency response**



In order to convolve the filter with a real signal in time domain was needed to implement the impulse response of the filter by applying the Inverse Fast Fourier Transform (IFFT), showed in figure 7.4.

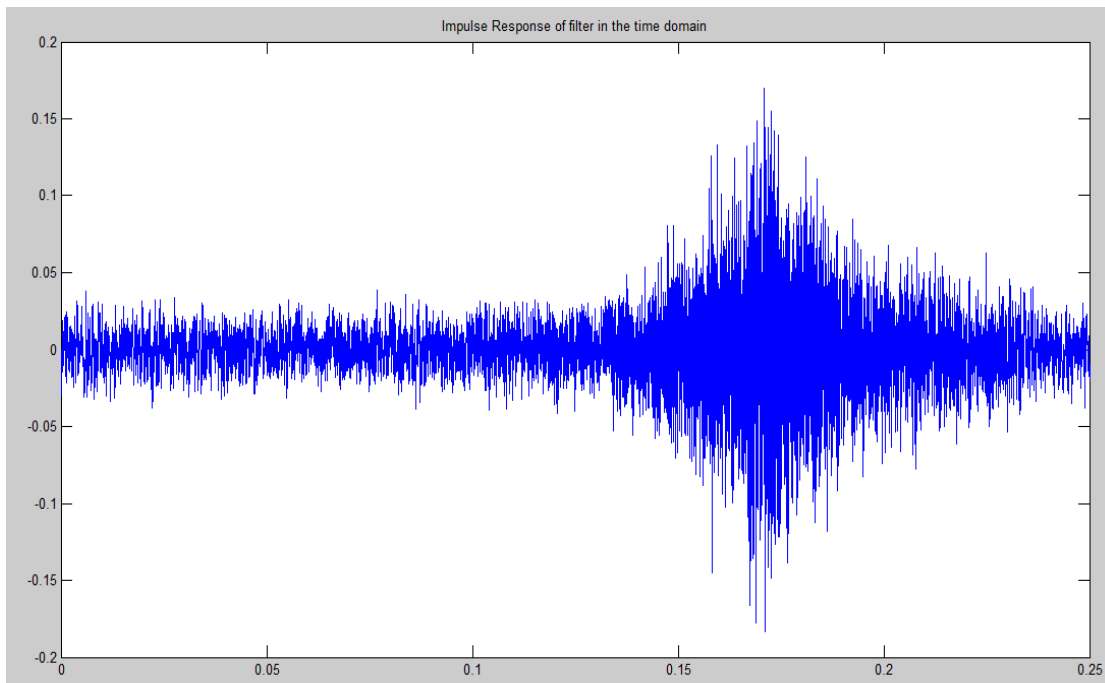


**Fig. 7.4: Designed filter impulse response**

Finally, in figure 7.5 it can be seen the frequency response of the improved tweeter after applying the filter. It can be notice a strong improvement especially from 1450Hz onwards.

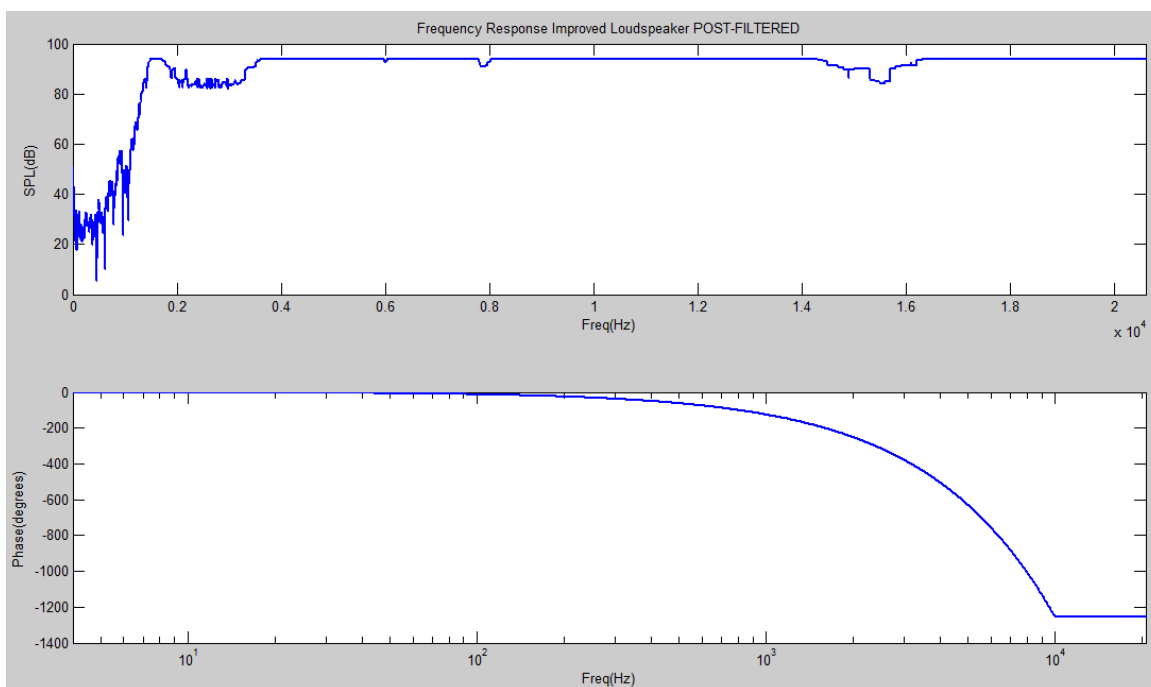


**Fig. 7.5: Post-processing frequency response**

## 8. Conclusions

In this section, conclusions about improving sound quality of piezoelectric loudspeaker are exposed.

### 8.1. Acoustic measurements

From the acoustic measuring process some important conclusions were drawn. By comparing the original-state-loudspeaker frequency response and the measurements taken after each modification, several theoretical concepts about loudspeakers were demonstrated.

Next table shows some observations about the different measurements and their importance for drawing conclusions.

**Table 8.1: Observations about the acoustic measurements**

Figures	Evaluation	Observations
5.5 vs 5.6	Horn influence in directivity	Horn has been well designed to control the directivity of the speaker. Polar diagram is more regular and symmetric respect $0^\circ$ with the horn.
5.4 vs 5.7	Back lid effect	Lid produces a higher output sound pressure level (SPL), mainly until 6kHz; but also introduces some undesirable reflections and irregularities in the response (sharper troughs and peaks).
5.8 vs 5.9	Horn effect in SPL	Horned configuration gives a much bigger SPL. This means that the horn compresses the air inside the speaker and that it has not only directional effects. It will be important to ensure the enclosure when modifications are performed in it.
5.3 vs 5.10	Damping material	The aim of damping material, such as cotton,

	inside the enclosure	is to attenuate the reflections from the back lid, the standing waves. <sup>[15]</sup> A smoother response is obtained but with no extraordinary results, due to the small size of the enclosure which does not cause a big amount of reflections from the back or these are in inaudible frequency range (short wavelength).
5.7 vs 5.12	Influence of lid shape	The back lid is not flat but is slightly bent. This may cause that back radiations do return concentrated to the same point and some frequencies experience reinforcement. Some troughs become less noticeable with the flat back lid configuration such as the one between 5700Hz and 5950Hz.
5.7 vs 5.13	Influence of enclosure depth	It was studied the effect of changing the cabinet depth from the original 12.44mm to 55mm. By comparing the measurements it is noticeable that the response is more unsteady with the big enclosure as new troughs come up and also SPL decrease in low-frequency range. Beranek, 1986 demonstrates that undesirable effects occur at the frequency where the depth of the box approaches a quarter of wavelength <sup>[15]</sup> ; at this frequency the box acts as a resonator tube, and more power is radiated from the rear side of the loudspeaker than at other frequencies. In this experiment, this would happen at 8575Hz for the small enclosure and at 1560Hz for the big one. The shape of the original lid controls the rear vibration at 8575Hz and in the case of the big cavity, the SPL at 1560Hz is small enough to make the effect inaudible.
5.7 vs 5.17	Bass reflex	Bass-reflex was designed to improve the low-frequency response of the tweeter but did not succeed. Once again because the enclosure is too small for this kind of modifications. Bass-reflex is useful to tune the cabinet frequency of bigger speakers <sup>[5]</sup> .
5.3 vs 5.14	Front air chamber	The aim of this experiment was to demonstrate that the horn must be as close as possible to the membrane. Otherwise, as it can be seen in figure 5.14, a big distortion is produced due to the fact that the sound is not concentrated before enter into the horn.

5.4 vs 5.15	Back radiation	This experiment helped to understand the behaviour of the coated paper attached to the crystal. It was checked that the shape of the cone allows increase the SPL. However, speaker radiating from the back has a flatter response between 4kHz and 8kHz (trough at 6kHz is missing).
5.16	Free radiation of the crystal	In a step further into the investigation of the behaviour of the cone it was measured the response without this component. In figure 5.16 it can be seen that a lot of distortion comes up. Because the cone is in contact with the chassis of the driver and glued to the crystal, the easiest way of movement of the diaphragm is up and down (the desirable direction). It can be concluded that the cone controls horizontal vibration of the crystal.
5.3 vs 5.19	Horizontal vibration control, naked loudspeaker	In order to minimise the horizontal movement and remove some undesirable distortion the rear suspension shown in figure 5.18 a & b was designed. Figure 5.19 shows a remarkable improvement of the SPL in low-frequency range (from 1585Hz onwards).

#### Conclusions,

- The horn is well-designed to control the directivity of the speaker. In addition, it has been proved that the location of this part (stuck to the membrane) is crucial to get a non-distorted response (concentrating the waves in its throat) and an increment in the SPL (by compressing the air inside the cavity).
- Modifications in the enclosure, such as introducing damping material or varying the depth, do not have noticeable results due to the small size of the enclosure. It is necessary to provide the tweeter of a small and hermetic cavity in order to compress the air in it and produce a high sound pressure level. It was checked that damping material inside the cavity gets a smoother response.
- The most effective and successful modifications are the ones carried out over the piezoelectric diaphragm. Because the small number of active

parts that this loudspeaker has (only a suspended crystal vibrating by its intrinsic properties) any modification of the way that the crystal is fixed to the chassis will be strongly reflected in the output frequency response.

Measurements show the positive effects of providing the piezoelectric diaphragm of a rear suspension that fixes the coated paper cone not only to the crystal, but also the chassis in order to guide its movement along only the vertical axis and maintain it centralised within the throat of the horn.

The next figure shows the original frequency response of the speaker and the response after the most successful improvement (providing the driver with a rear suspension). As a reference, frequency 1584Hz has been marked with a cursor in both responses. In the original speaker the SPL at that frequency is 73.864dB and 87.055dB in the modified.

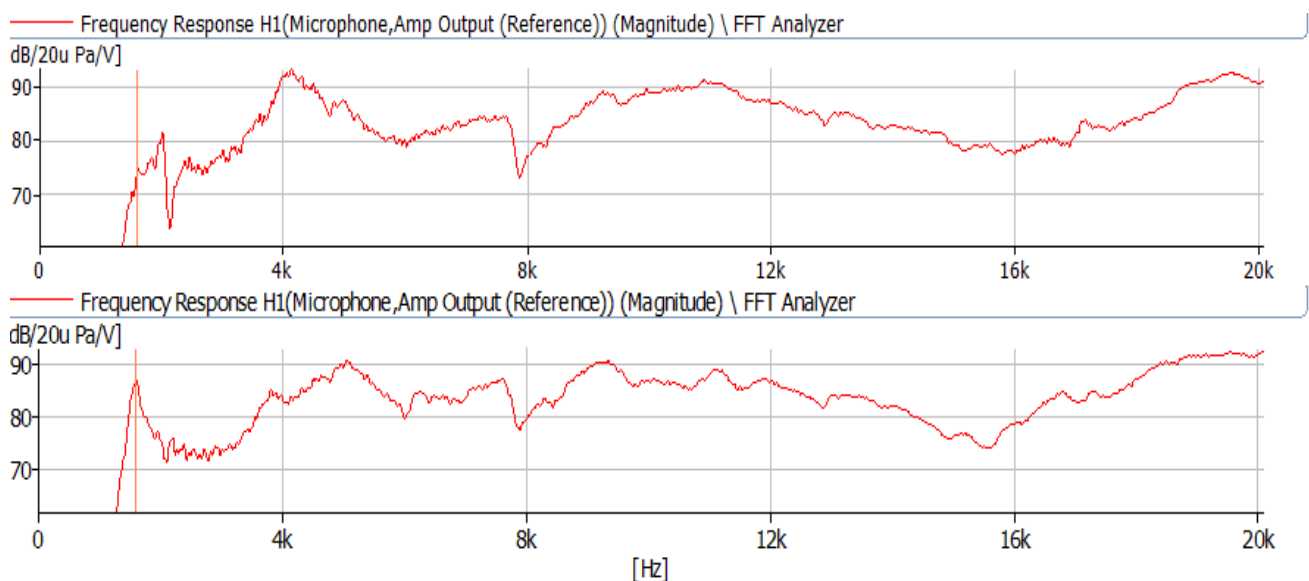


**Fig. 8.1: Complete loudspeaker before (up) and after (down) modifications**

## 8.2. Electroacoustic measurements

Electroacoustic characterisation consisted of measuring the resonant frequency of naked, complete and modified loudspeaker configurations through electric admittance.

In addition, it was demonstrated that, as stated in the equation 2.1, the frequency of resonance of the speaker is inversely proportional to the square root of the weight of the diaphragm. By comparing figures 5.20 and 5.22 and the measured frequencies ( $f_{0em}=2840\text{Hz}$  and  $f_{0em}=1928\text{Hz}$ , respectively) it can be checked that the resonance frequency is lower when the 5p coin is glued to the cone. The aim of the experiment was accomplished although the coin cannot stay glued to the diaphragm due to its excessive weight causes acoustic distortion in the output.

The experience gained with this experiment was used in the acoustic modification as the rear suspension acts as an added mass to the diaphragm. Thus, comparing figures 5.21 and 5.23 it can be seen that resonance frequency go down from 3716Hz in non-modified loudspeaker to 1604Hz in complete tweeter provided with rear suspension. This fact is also reflected in figure 8.1 as an increment in the sound pressure level up to 4kHz.

### 8.3. Laser measurements

By comparing figures 6.4 to 6.7 it is noticeable that, despite selecting points symmetrically placed, with respect to the central point, the shape of the measurements is quite different. Similarities can be observed between figures 6.5 and 6.7 and between figures 6.6 and 6.8. This suggests that the diaphragm has an average pattern of vibration like the one illustrated in the figure 8.2.

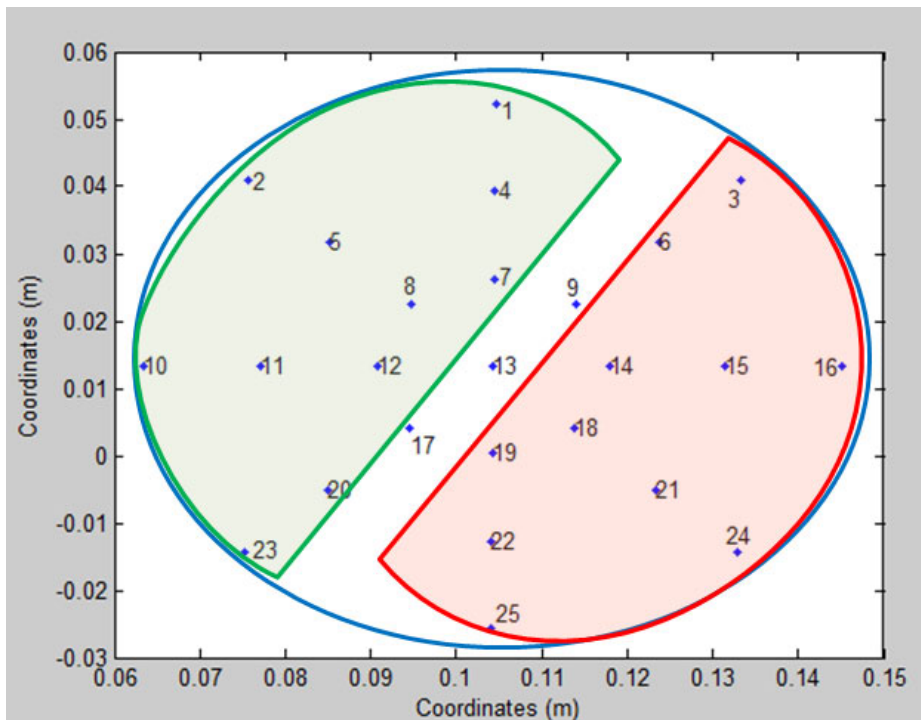
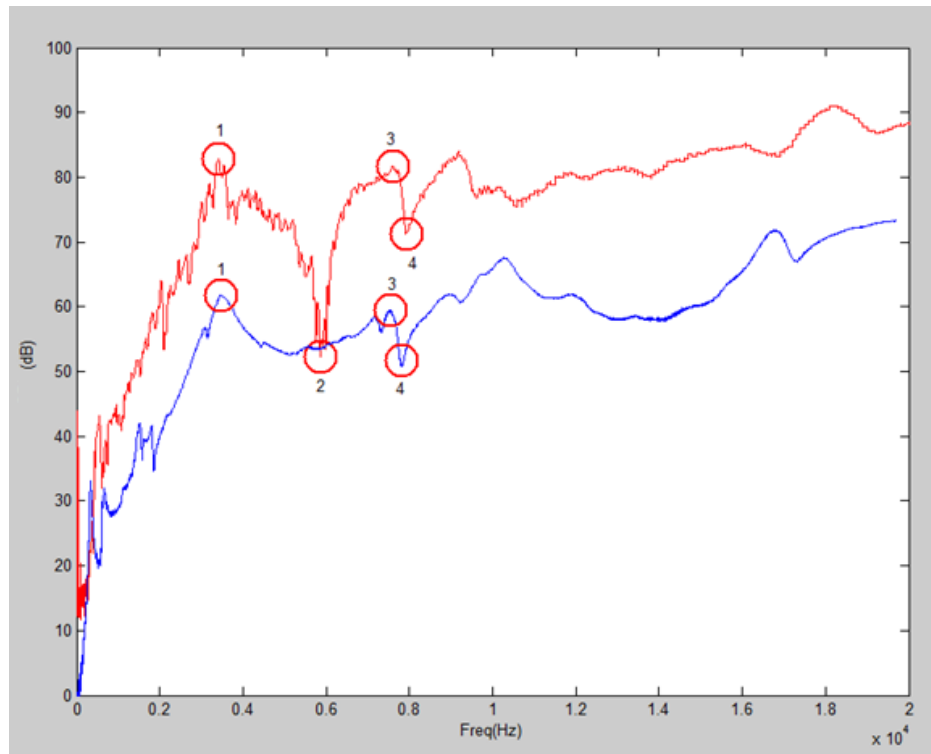


Fig. 8.2: Zones of the diaphragm with similar behaviour

The points with the same colour have a similar behaviour with the frequency but that does not mean that they move with the same amplitude at the same time (in that case the sound would be cancelled).

The next image shows the frequency response (red) and the acceleration measurement taken with the laser (blue). A relationship between them has been sought. The amplitude difference is not important as different magnitudes are being measured.



**Fig. 8.3: Frequency response (red) and acceleration of the diaphragm (blue)**

Points 1, 3 and 4 of figure 8.3 are easily comparable in both measurements. This suggests that the average acceleration in the 25 points present those irregularities, possibly because of a structural issue. In points 1 and 3 the reason may be that at one of those frequencies the piezoelectric crystal presents its mechanical resonance frequency and the harmonic of this one, i.e. the frequency in which the crystal vibrates more easily, which causes the whole diaphragm to enhance those frequencies. Also, it has to be considered the way the crystal is fixed to the chassis because, as it was seen in the acoustic experiments, a small change in the two wires that suspend it causes strong changes in the frequency response.

The software of *Polytec Vibrometer Scanning* allows plotting 2D and 3D representations of the response in a specific frequency. This tool is used to illustrate the vibration at 3408Hz (point 1) and also to find an accurate explanation to the big trough at point 2 (5856Hz).



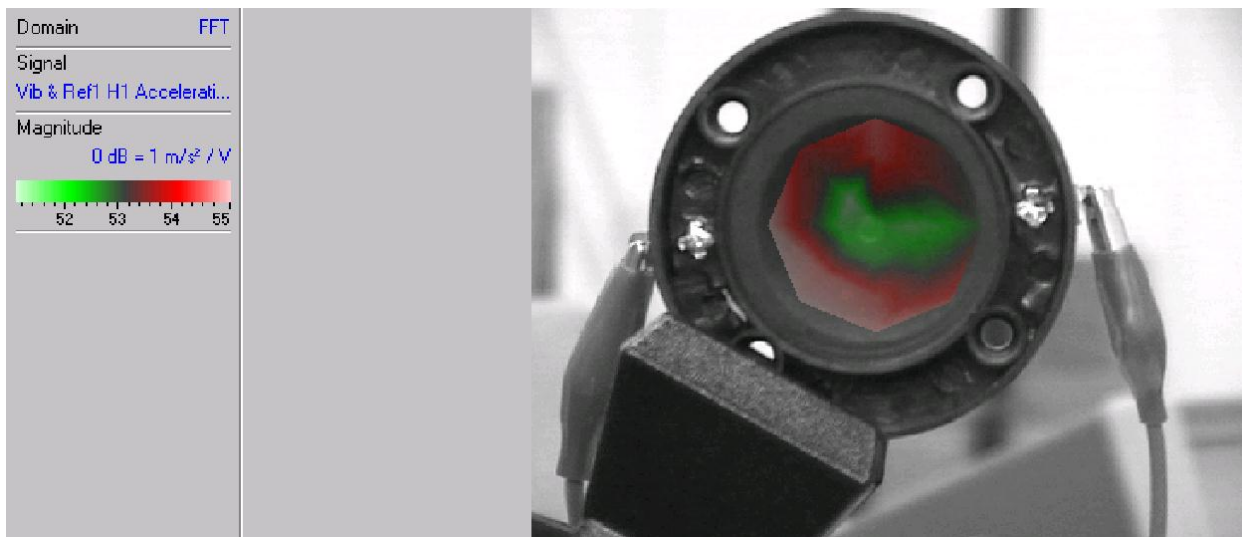


**Fig. 8.4: 2D plot of laser scanner at 3408Hz**



**Fig. 8.5: 2D plot of laser scanner at 5856Hz**

It is noticeable that the pattern of vibration of both points is completely different as the first one corresponds to a peak and the second one corresponds to a trough.

The figure 8.5. indicates that at the frequency under review (5856Hz) the diaphragm has a rocking movement, instead of vibrating flat, as a piston. This pattern of movement produces a cancelation in terms of sound radiation. Although the crystal is moving, the sound that is produced by half of the crystal is cancelled by the opposite movement of the other half. This conclusion can be extrapolated to the point 4.

To sum up, from the measurements taken with the scanning laser, it can be concluded that the loudspeaker has a structural problem in the way the

piezoelectric diaphragm is fixed to the chassis. Therefore, the paper cone has not a symmetric vibration and hence, it presents irregularities in the acoustic output signal. Furthermore, at some frequencies the diaphragm presents a rocking movement that provokes several troughs in the frequency response. This problem strengthens the need of equipping the speaker with an effective rear suspension that fixes the coated paper cone to the chassis, guides the vibrations along only the vertical axis and keep the crystal centred.

## 8.4. Inverse filter

After Matlab implementation, a new session of measurements was performed in the small anechoic chamber in order to verify the proper functioning of the filter. The frequency response of the complete tweeter was measured again and the data was introduced into Matlab to design the inverse filter.

The next figures correspond to the Pulse measurements: frequency response with the filter deactivated and activated, respectively.

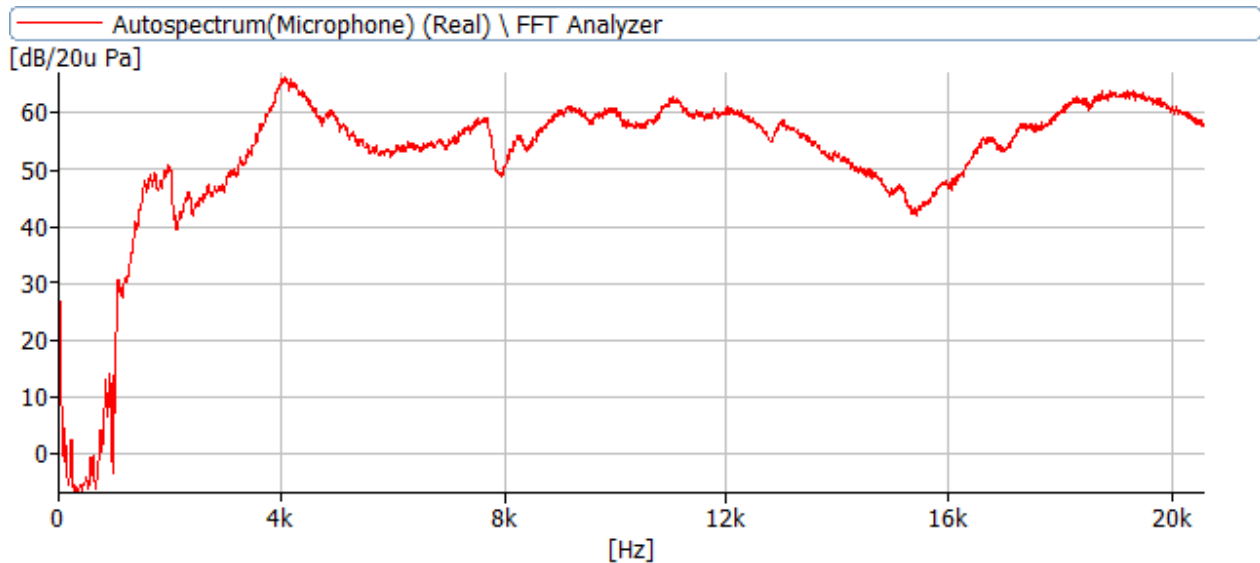


Fig. 8.6: Measured frequency response, inverse filter OFF

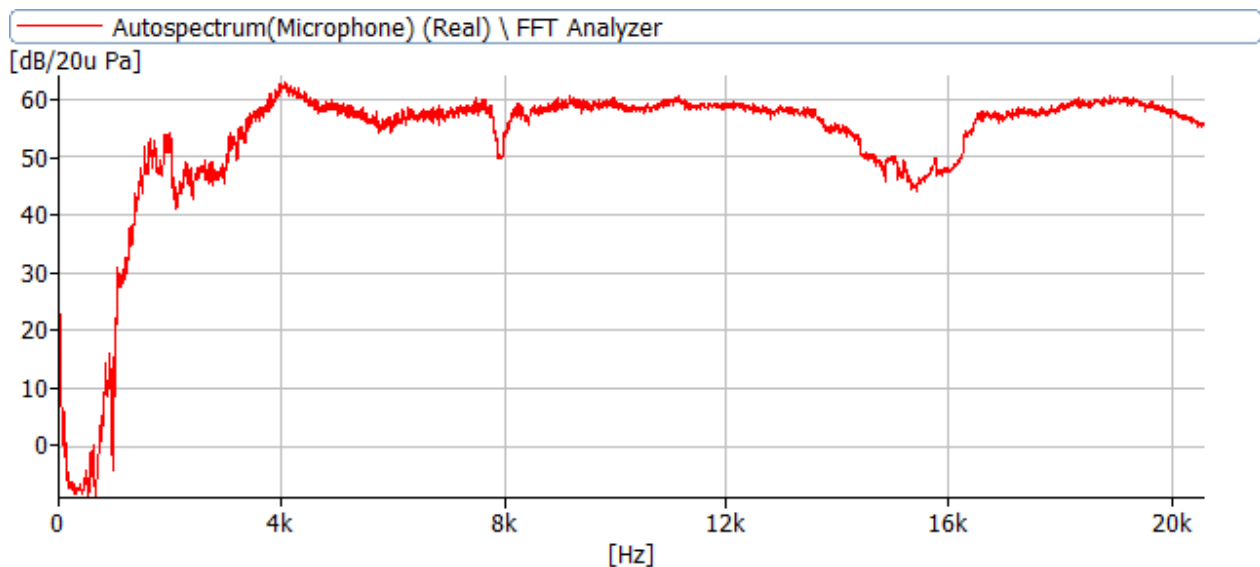


Fig. 8.7: Measured frequency response, inverse filter ON

By comparing figures 8.6 and 8.7 it is noticeable that the aim of the filter is accomplished since a flatter and smoother response in the output signal is reached. Some of the troughs remain due to the limitation set in the amplification amplitude to avoid a possible destruction of the speaker.

## 9. References

- [1] NEWEL, PHILIP; KEITH R. HOLLAND (2007), *Loudspeakers: for music recording and reproduction*, 1<sup>st</sup> edition, Amsterdam: Elsevier, Focal Press.
- [2] PIEZO SYSTEMS (2013), *History of Piezoelectricity*. Available from: <http://www.piezo.com/tech4history.html> [Accesed Dec 2013]
- [3] MURATA MANUFACTURING COMPANY Ltd. (2012), *Piezoelectric Sound Components, P15E-8*; Japan: Application Manual.
- [4] BASILIO PUEO ORTEGA Y MIGUEL ROMÁ ROMERO (2003), *Electroacústica, Altavoces y Micrófonos*, Madrid: Prentice Hall.
- [5] EARGLE, J. (2003), *Loudspeaker Handbook*, 2<sup>nd</sup> edition, Boston: Kluwer Academic.
- [6] ROSING, T. D. (2000), *Science of Percussion Instruments*, 1<sup>st</sup> edition, Singapore: World Scientific.
- [7] EMINENCE (2014), *Understanding Loudspeaker Data*. Available from: <http://www.eminence.com/support/understanding-loudspeaker-data/> [Accesed February 2014]
- [8] KINSLER, LAURENCE E.; FREY, AUSTIN R.; COPPENS, ALAN B. and SANDERS, JAMES V. (2000), *Fundamentals of Acoustics*, 4<sup>th</sup> edition, New York: John Wiley & Sons.
- [9] COLLOMS, M. (2005), *High Performance Loudspeakers*, 6<sup>th</sup> edition, Chichester: John Wiley & Sons.

- [10] SÁNCHEZ BOTE, J.L.; GÓMEZ ALFAGEME, J.J.; ÁLVAREZ FERNÁNDEZ, E.; DEL POZO CALVO, H. (2005), *Laboratorio de Electroacústica*, 1<sup>st</sup> edition, Madrid: Dpto. Publicaciones EUITT.
- [11] ROSSI, M. (1988), *Acoustics and electroacoustics*, 1<sup>st</sup> edition, Norwood: Artech House.
- [12] HYE, J. K. *et al* (2012), *Improvement of Low-Frequency Characteristics of Piezoelectric Loudspeakers Based on Acoustics Diaphragms*, Research paper, IEEE Transactions on Ultrasonics, Ferroelectrics, and Frequency Control, Vol. 59, No 9.
- [13] HYE, J. K. *et al* (2009), *High Performance Piezoelectric Microspeakers and Thin Speaker Array System*, Research paper, ETRI Journal, Vol. 31, No 6.
- [14] OLE KIRKEBY *et al* (1996), *Local sound field reproduction using digital signal processing*, Research paper, Acoustical Society of America, Vol. 100, No 3.
- [15] BARANEK, LEO L. (1986), *Acoustics*, 2<sup>nd</sup> edition, New York: American Institute of Physics for the Acoustical Society of America.

# APPENDICES

## APENDIX A1: Inverse filter Matlab script

```
clear;clc;close all;

%*****
% Name:      inversefilter.m
% Author:    Javier Fernandez Martinez - Individual Project
% Date:      May 2014
%*****

%% Get in Matlab loudspeaker frequency response from Pulse data
(magnitude and phase) - FR59
[sample2,freq2,absTF,cTF]=textread('response2.txt','%f %f %f %f');
freq2=freq2./1000000;
absTF=absTF./1000000;
cTF=cTF./1000000;
fs=2*max(freq2);

%TF=2e-5*10.^(absTF/20);
TF=absTF.*exp(-1i*cTF);
TF=TF/max(abs(TF));

%% Original frequency response
figure,subplot 211
plot(freq2,20*log10(abs(TF/(2e-5))), 'LineWidth',2);
semilogx(freq2,20*log10(abs(TF/(2e-5))), 'LineWidth',2);
title('Frequency Response Improved Loudspeaker (FR59)');
xlabel('Freq(Hz)');
ylabel('SPL (dB)');
xlim([freq2(1) 20600]);
ylim([0 100]);

subplot 212
plot(freq2,unwrap(angle(TF)), 'LineWidth',2);
xlabel('Freq(Hz)');
ylabel('Phase (degrees)');
xlim([freq2(1) 20600]);
ylim([-8000 2000]);

%% Creation of the filter in the time domain
H=zeros(size(freq2));
rep=zeros(size(freq2));

a=1;
dt=1/max(freq2);
betaR=logspace(-20,10,100); % Define regularisation coefficients

for ci=1:length(freq2)
    effort=12;
    w=2*pi*freq2(ci);
    a=exp(-1i*w*(512)*dt);%target function. 512 is for providing the
    number with a phase

    counter_beta=1; %(when beta go up, effort go down)

    while effort>=12 && counter_beta<length(betaR)&& w~=0 %Set the max
    amplification (<=12dBV)

        H(ci)=(TF(ci)'*TF(ci)+betaR(counter_beta))\ (TF(ci)'*a);
```

```

        effort=10*log10(abs((H(ci)'*H(ci))));

        counter_beta=counter_beta+1;
    end
end
%%
figure
subplot 211
plot(freq2,20*log10(abs(H)), 'LineWidth',2);
title('Frequency Response of Filter');
xlim([0 20600]);
ylim([0 13]);
xlabel('Freq(Hz)');
ylabel('|H| Gain (dBV)');

subplot 212
semilogx(freq2,unwrap(-angle(H)), 'LineWidth',2);
title('Phase of the filter');
xlabel('Freq(Hz)');
ylabel('Phase H (degrees)');
xlim([freq2(1) 20600]);
ylim([-8000 2000]);

%% Post-filtered

rep=TF.*(H);

figure
subplot 211
plot(freq2,20*log10(abs(rep)/(2e-5)), 'LineWidth',2);
title('Frequency Response Improved Loudspeaker: FILTER ON');
xlabel('Freq(Hz)');
ylabel('SPL(dB)');
xlim([freq2(1) 20600]);

subplot 212
semilogx(freq2,unwrap(angle(rep)), 'LineWidth',2);
xlabel('Freq(Hz)');
ylabel('Phase(degrees)');
xlim([freq2(1) 20600]);

%% Impulse response of the source and the filter

IRq=ifft([TF; flipud(conj(TF(2:end)))]);
figure
plot((1:length(IRq))/(max(freq2)),IRq)
title('Impulse Response of the source')

% reconstructed=fft(IRq);
% figure
% plot(1:length(reconstructed),20*log10(abs(reconstructed)))

Q=[H ;conj(flipud(H(2:end)))]; %ordenando el filtro para poder hacer la
IFFT
IR_filtro=ifft(Q);
% IR_filtro=ifft(H,'symmetric');
figure
plot((1:length(IR_filtro))/(fs),IR_filtro);
xlim([0 0.25]);
title('Impulse Response of filter in the time domain')

```

```

%% Periodogram

noise_vect=randn(1,30*fs);
[noise_f,fp]=periodogram(noise_vect,[],2048,fs);
% figure
% plot(fp,10*log10(noise_f),'linewidth',2)
% hold on

white_conv=filter(IRq,1,noise_vect);
[white_conv_f,fp]=periodogram(white_conv,[],2048,fs);
% plot(fp,10*log10(white_conv_f),'k','linewidth',2)

white_filtered=filter(IR_filtro,1,white_conv);
[white_filtered_f,fp]=periodogram(white_filtered,[],2048,fs);

% plot(fp,10*log10(white_filtered_f),'r','linewidth',2)
% legend('Noise','Speaker output','Filtered output')
% xlim([100 fs/2])

%%
filtered_output=filter(IR_filtro,1,noise_vect);
%sound (wgn(15*fs,1,0),fs);
sound(filtered_output,fs)

```